

A STUDY OF GAS SOLUBILITIES AND TRANSPORT
PROPERTIES IN FUEL CELL ELECTROLYTES

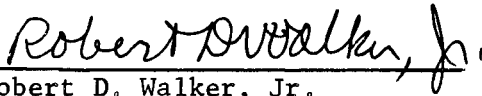
Research Grant NGR 10-005-022

Fourth Semi-Annual Report

Period Covered: March 1, 1967 - August 31, 1967

Prepared For
National Aeronautics and Space Administration
Washington, D. C.

October 9, 1967


Robert D. Walker, Jr.
Principal Investigator

ENGINEERING AND INDUSTRIAL EXPERIMENT STATION

College of Engineering
University of Florida
Gainesville, Florida

TABLE OF CONTENTS

	<u>Page</u>
LIST OF TABLES.....	iii
LIST OF FIGURES.....	iv
SUMMARY.....	1
1.0 INTRODUCTION.....	3
2.0 SOLUBILITY OF GASES IN POTASSIUM HYDROXIDE SOLUTIONS...	4
2.1 Experimental.....	4
2.1.1 Saturation Test.....	4
2.2 Results.....	5
2.2.1 Solubility of Oxygen.....	7
2.2.2 Solubility of Hydrogen.....	11
2.2.3 Solubility of Argon.....	11
2.3 Discussion.....	11
2.3.1 Partial Molal Heats of Solution.....	12
2.3.2 Entropy of Solution.....	13
2.3.3 Energy of Solution.....	20
3.0 THE DIFFUSIVITY OF OXYGEN AND HYDROGEN IN KOH SOLUTIONS	28
3.1 Experimental.....	29
3.1.1 Theory.....	29
3.1.2 Procedure.....	31
3.2 Results and Discussion.....	33
4.0 DIFFUSION OF WATER IN POTASSIUM HYDROXIDE SOLUTIONS....	39
4.1 Results.....	39
4.2 Theory.....	42
4.3 Discussion.....	45

	<u>Page</u>
5.0 LITERATURE SURVEY OF PROPERTIES OF LITHIUM HYDROXIDE SOLUTIONS.....	51
6.0 FUTURE PLANS.....	52
APPENDIX 1.....	53
REFERENCES.....	58
APPENDIX II.....	Attached

LIST OF TABLES

<u>Table</u>	<u>Page</u>
2.1 Solubility of Non-Polar Gases in Aqueous Potassium Hydroxide Solutions.....	6
4.1 Integral Diffusion Coefficients of Aqueous KOH Solutions.....	40
4.2 Differential Diffusion Coefficients of Aqueous KOH Solutions.....	41
A.1.2 Solubility of Lithium Hydroxide in Water.....	53
A.1.3 Vapor Pressure of LiOH Solutions.....	54
A.1.4 Vapor Pressure of Solid $\text{LiOH} \cdot \text{H}_2\text{O}$	54
A.1.5 Heat Capacity of Aqueous LiOH Solutions at 20°C.....	55
A.1.6 Viscosity of LiOH Solutions.....	55
A.1.7 Density of LiOH Solutions.....	56
A.1.8 Electrical Conductivity of LiOH Solutions.....	56
A.1.9 Properties of Solid Lithium Hydroxide.....	57

LIST OF FIGURES

<u>Figure</u>	<u>Page</u>
2.1 Solubility of Oxygen in Aqueous Potassium Hydroxide Solutions.....	8
2.2 Solubility of Hydrogen in Aqueous Potassium Hydroxide Solutions.....	9
2.3 Solubility of Argon in Aqueous Potassium Hydroxide Solutions.....	10
2.4 Henry's Law Constant for O ₂ -Aqueous KOH System.....	14
2.5 Henry's Law Constant for H ₂ -Aqueous KOH System.....	15
2.6 Henry's Law Constant for Ar-Aqueous KOH System.....	16
2.7 Heats of Solution for O ₂ -Aqueous KOH System.....	17
2.8 Heats of Solution for H ₂ -Aqueous KOH System.....	18
2.9 Heats of Solution for Ar-Aqueous KOH System.....	19
2.10 Entropies of Solution for O ₂ -Aqueous KOH System.....	21
2.11 Entropies of Solution for H ₂ -Aqueous KOH System.....	22
2.12 Entropies of Solution for Ar-Aqueous KOH System.....	23
2.13 Energies of Solution for O ₂ -Aqueous KOH System.....	25
2.14 Energies of Solution for H ₂ -Aqueous KOH System.....	26
2.15 Energies of Solution for Ar-Aqueous KOH System.....	27
3.1 Schematic Diagram of Linear Diffusion in a Stagnant Cell.....	30
3.2 Diffusivity of Oxygen in Potassium Hydroxide Solutions at 25°C.....	34
3.3 Relationship of Diffusivity of Oxygen to Species Fraction of Potassium Hydroxide.....	36
3.4 Diffusivity of Hydrogen in Potassium Hydroxide Solutions at 25°C.....	38
4.1 Diffusion coefficients of Aqueous KOH Solutions.....	46
4.2 Log D versus T ⁻¹ for Aqueous KOH Solutions.....	47
4.3 Relative Diffusion Coefficients D ^{id} /D ^o for Aqueous KOH Solutions at 25°C.....	49
4.4 Diffusion Coefficients of Aqueous KOH Solutions at 25°C	50

Summary

This report describes work done on (1) the solubility of hydrogen and oxygen in KOH solutions, (2) the diffusivity of oxygen in KOH solutions, (3) the mutual diffusivity of water and KOH, and (4) a summary of pertinent data for the $\text{LiOH-H}_2\text{O}$ system.

The solubility of oxygen, hydrogen, and argon have been determined for the KOH concentration range of 0 to approximately 50 wt %, and up to a temperature of 80°C . The solubility of each of these gases decreases sharply with KOH concentration and somewhat less sharply with increasing temperature. Henry's law constants show little variation with temperature but are strongly dependent on KOH concentration. Heats of solution, entropies of solution, and energies of solution have been derived from the solubility data, and all of these show generally strong dependence upon both temperature and KOH concentration. For the most part, the values of the thermodynamic properties are negative, but there are a number of cases where the sign changes to positive. In general, the numerical value of the heats and energies of solution is less than -3.0 Cal./g.mole .

The diffusivity of oxygen in KOH solutions at 25°C has been determined for four KOH concentrations. The values reported here are generally somewhat lower (about 10%) than values in the literature; however, extrapolation to infinite dilution leads to a value of $1.91 \times 10^{-5} \text{ cm}^2/\text{sec}$, which is very close to the generally accepted value of the diffusivity of oxygen in water at 25°C .

The mutual diffusivity of water and KOH has been measured for the KOH concentration range 0-10 N, and for the temperature range $25-75^\circ\text{C}$. The

dependence of the diffusion coefficient on KOH concentration is complex, tending to pass through a minimum at about 0.25 N, and then through a maximum at about 4-5 N. A theoretical treatment, based on perturbation of the activation energy for diffusion by surrounding ions, has been developed; the experimental data agree well with its predictions over the whole concentration range, whereas the Onsager-Fuoss treatment deviates sharply from the experimental data at KOH concentrations greater than about 0.25 N.

Pertinent literature data on the $\text{LiOH-H}_2\text{O}$ system are also summarized in this report.

1.0 Introduction

This report covers work involving the following: (1) additional measurements of the solubility of hydrogen and oxygen in KOH solutions, (2) measurements of the mutual diffusivity of water and KOH, (3) measurements of the diffusivity of oxygen in KOH solutions, and (4) a summary of pertinent data for aqueous solutions of lithium hydroxide.

For the most part, the work on solubility of gases in the temperature and concentration ranges of interest was completed during the past six months. A few measurements at the higher temperatures are still incomplete, but sufficient data are now in hand to enable one to characterize the solubility of non-polar gases in aqueous KOH solutions reasonably well.

Similarly, the work on the mutual diffusivity of water and KOH has been essentially completed during this period.

Few measurements of the diffusivity of either hydrogen or oxygen in KOH solutions were made during earlier periods. During the past six months, however, intensive work by a graduate student has resulted in an experimental technique which seems to be yielding good results. A few diffusivities of oxygen in KOH solutions are reported here.

Finally, work has begun on the solubility and diffusivity of oxygen and hydrogen in aqueous LiOH. For the most part this has consisted of assembling pertinent data from various published sources.

2. SOLUBILITY OF GASES IN POTASSIUM HYDROXIDE SOLUTIONS - S. K. Shoor

Solubility of oxygen, hydrogen and argon in aqueous potassium hydroxide solutions have been measured at temperatures of 25, 40, 60 and 80°C. Measurements for H₂ have also been made at 100°C.

2.1 Experimental

The method previously used for measurements of oxygen solubility, described in detail in the 2nd Semi-Annual Report (1) involved concentration of the oxygen by adsorption on a column immersed in liquid nitrogen. This method was not suitable for measurements of hydrogen solubilities since hydrogen boils at a temperature below that of any of the gases which can be used as chromatograph carrier gases, and was therefore not quantitatively adsorbed. Because of this, hydrogen, after being stripped from the stripping cell, could not be effectively adsorbed. Consequently hydrogen solubilities were measured by the method used by Gubbins and Walker (2). The method was essentially the same as described in the 1st Semi-Annual Report (3) except that the stripping cell was redesigned so that larger samples could be injected without appreciable backmixing in the cell. Earlier measurements involved the use of a stripping cell of 3 cm. diameter; however, in these measurements appreciable backmixing in the gas space above the liquid sample led to an unacceptable broadening of the chromatograph peak. To overcome this problem a stripping cell 1 cm. in diameter and 450 cm. long was constructed. This method was also used to determine argon solubilities, and to determine oxygen solubilities.

2.1.1 Saturation Test

An accurate knowledge of the partial pressure of the solute gas in the saturation vessel is essential for reliable solubility measurements.

The gas, therefore, was passed through a set of presaturators before entering the main saturating vessel. In this way the partial pressure of the solute could be determined from the known atmospheric pressure and vapor pressure of the KOH solution.

To check that the gas entering the saturation vessel was fully saturated, the following saturation test was conducted. The vapors emerging from the saturating vessel were collected for a known period of time in a U-tube containing Drierite. From the weight of water collected and the flow-rate of the gas, the degree of saturation was determined.

Such tests showed that the gas was not fully saturated, especially at higher temperatures, and this fault was traced to condensation of vapor in the tubing connecting the presaturators. This was overcome by heating the tubing.

Since the oxygen solubilities reported earlier were obtained before these tests were conducted, the values may be in error due to discrepancies in the assumed partial pressure values. For this reason the oxygen measurements given in the 2nd and 3rd Semi-Annual Reports have been repeated using presaturators with heated connecting tubing.

2.2 Results

The experimental data for the solubility of oxygen, hydrogen and argon have been tabulated in Table 2.1. The errors attached to the solubility values in Table 2.1 are the standard deviations from the arithmetic mean. In almost all cases the solubilities are the mean values for 4 or more replicate measurements. The absolute accuracy of the reported data depends on the KOH concentration, being less at high concentrations. Comparison of values of the solubility for pure water reported here with

Table 2.1

Solubility of Non-Polar Gases in Aqueous Potassium Hydroxide Solutions

Gas	Wt % KOH	Solubility at 25°C g.mole/l. x 10 ⁻³	Solubility at 40°C g.mole/l. x 10 ⁻³	Solubility at 60°C g.mole/l. x 10 ⁻³	Solubility at 80°C g.mole/l. x 10 ⁻³	Solubility at 100°C g.mole/l. x 10 ⁻³
O ₂	0	1.263(Lit. value)	1.049±0.007	0.875±0.009	0.786(Lit. value)	
	5.00	0.825±0.007	0.684±0.006	0.605±0.008	0.584±0.005	
	13.50	0.413±0.007	0.365±0.007	0.339±0.003	0.315±0.004	
	23.00	0.155±0.002	0.145±0.0015	0.139±0.001	0.137±0.002	
	31.60	0.0613±0.0007	0.0589±0.0014	0.056±0.001	0.055±0.002	
	40.70	0.0179±0.0002	0.0197±0.0007	0.0193±0.004	0.0196±0.0007	
	50.30	-	0.00563±0.0002	-	-	
	50.65	0.0055±0.0001	-	0.00540±0.0002	0.0055±0.0003	
H ₂	0	0.792±0.006	0.713±0.014	0.712±0.0076	-	-
	5.00	0.583±0.005	0.560±0.005	0.540±0.007	0.539±0.008	-
	9.00	0.465±0.004	0.435±0.014	0.410±0.003	0.394±0.007	-
	19.50	0.226±0.003	0.217±0.005	0.199±0.005	0.196±0.005	-
	32.40	-	0.082±0.003	0.078±0.002	0.079±0.002	-
	34.50	0.078±0.002	-	-	-	-
	38.00	-	-	-	-	0.0467±0.0013
	41.40	0.0384±0.002	0.0349±0.0012	0.0333±0.0006	0.033±0.002	0.0342±0.0009
Ar	52.40	0.011±0.001	0.0097±0.0064	0.0093±0.0005	0.0095±0.0004	0.0086±0.0004
	56.40	-	-	-	-	0.0066±0.0003
	0	1.407±0.007	1.122±0.003	0.919±0.004	-	-
	5.00	0.903±0.005	0.758±0.006	0.658±0.001	0.620±0.006	-
	13.50	0.442±0.002	0.400±0.003	0.355±0.002	0.334±0.002	-
	23.00	0.183±0.002	0.162±0.003	0.157±0.002	0.147±0.004	-
	31.60	-	-	0.064±0.002	0.061±0.002	-
	32.50	0.062±0.001	-	-	-	-
	36.60	-	0.036±0.001	-	-	-
	40.70	-	-	-	-	-
	41.40	0.0020±0.0007	0.0180±0.0006	0.0199±0.0007	0.0199±0.0009	-

literature values suggests that the accuracy of the data for dilute solutions is about $\pm 1.5\%$. The accuracy for concentrated solutions (of the order 50 Wt. % KOH) is difficult to estimate, but is believed to be of the order $\pm 6\%$.

The solubility values for oxygen and argon at all temperatures and that of hydrogen at temperatures of 25, 40 and 60°C have been plotted on a semilog paper with abscissa as potassium hydroxide concentration and ordinate as solubility in g.mole of the solute gas per liter of the solution. Figures 2.1, 2.2 and 2.3 show such plots. Since the solubility values obtained for hydrogen at temperatures of 80° and 100°C were very close to those at 60°C, they have not been plotted. Solid lines in these plots represent this work whereas the points indicate the work of previous investigators.

2.2.1 Solubility of Oxygen

In comparing the results for oxygen with those of other investigators it may be seen that at 25°C these data agree within a few percent with the data of Geffcken (4) and Tobias (5). At temperatures other than 25°C, the values reported by various workers differ appreciably. The disagreement is quite pronounced even at low KOH concentrations. For example, at 60°C the solubility reported by Tobias (5) in pure water differs significantly (by about 15%) from the currently accepted literature value (6), and this suggests that discrepancies may be present at other concentrations also. The solubilities reported here agree quite well with those reported by Knaster and Apelbaum at very low and very high KOH concentrations. However, at intermediate concentrations the disagreement is quite marked.

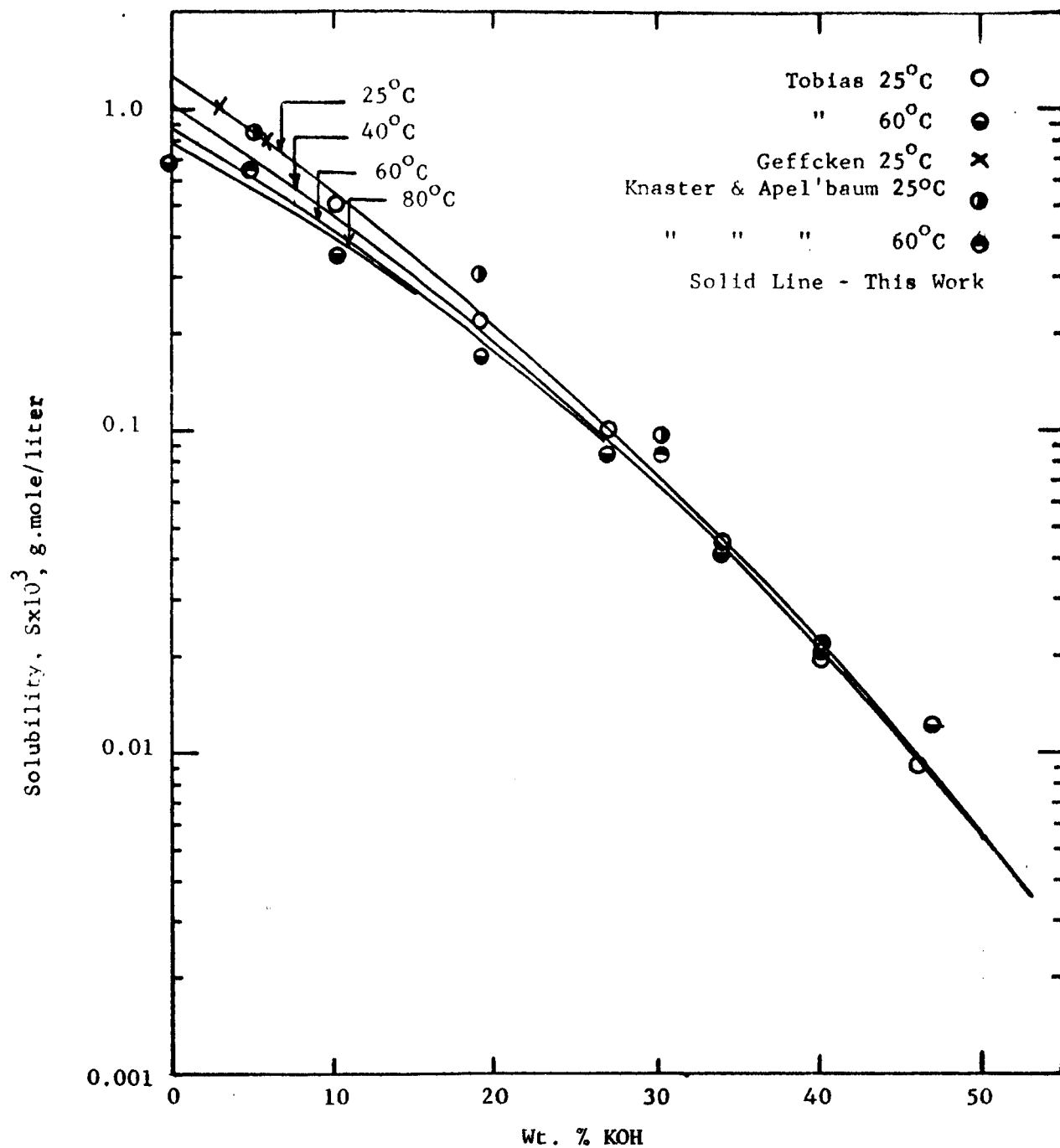


Figure 2.1 SOLUBILITY OF OXYGEN IN AQUEOUS POTASSIUM HYDROXIDE SOLUTIONS

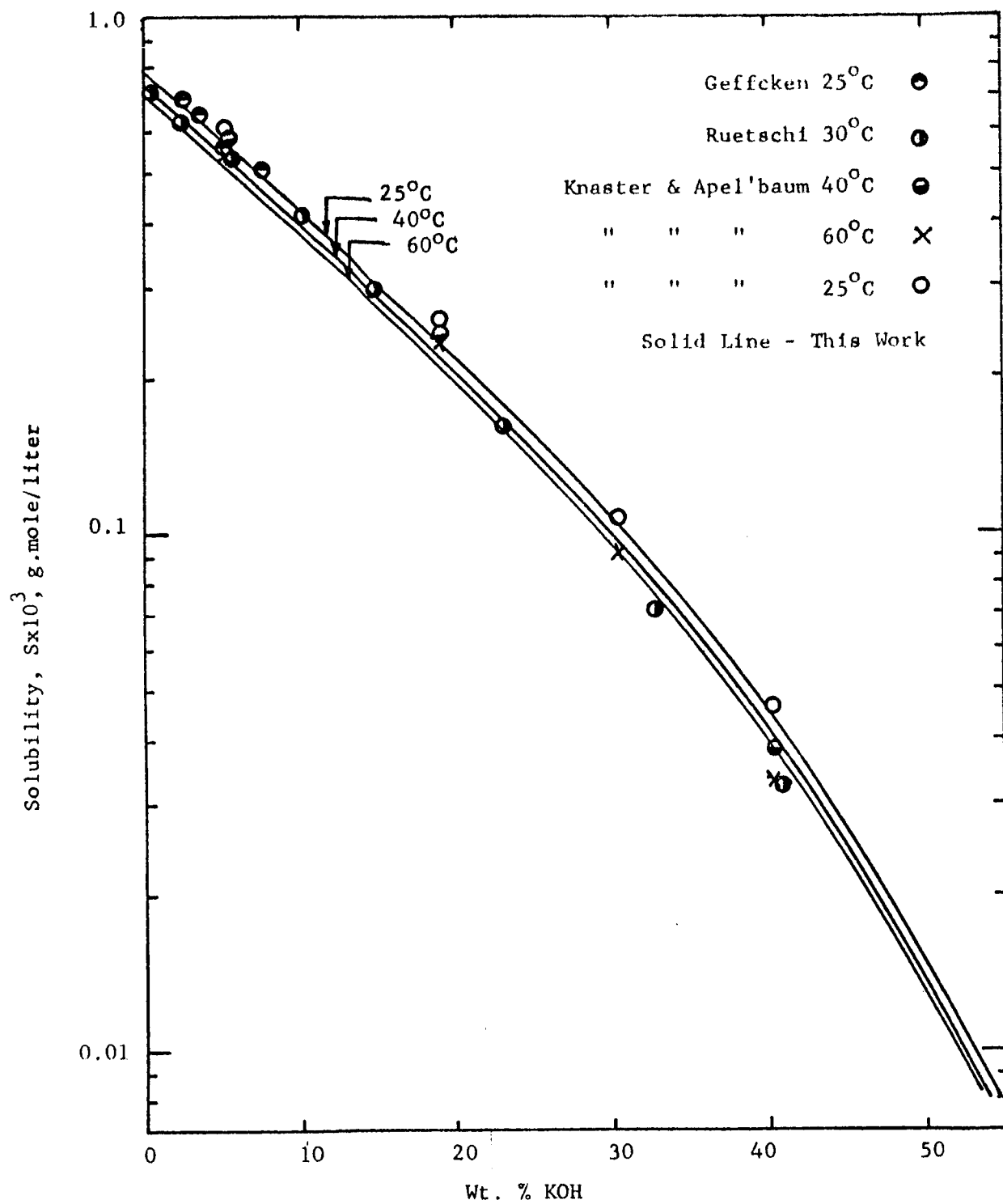


Figure 2.2 SOLUBILITY OF HYDROGEN IN AQUEOUS POTASSIUM HYDROXIDE SOLUTIONS

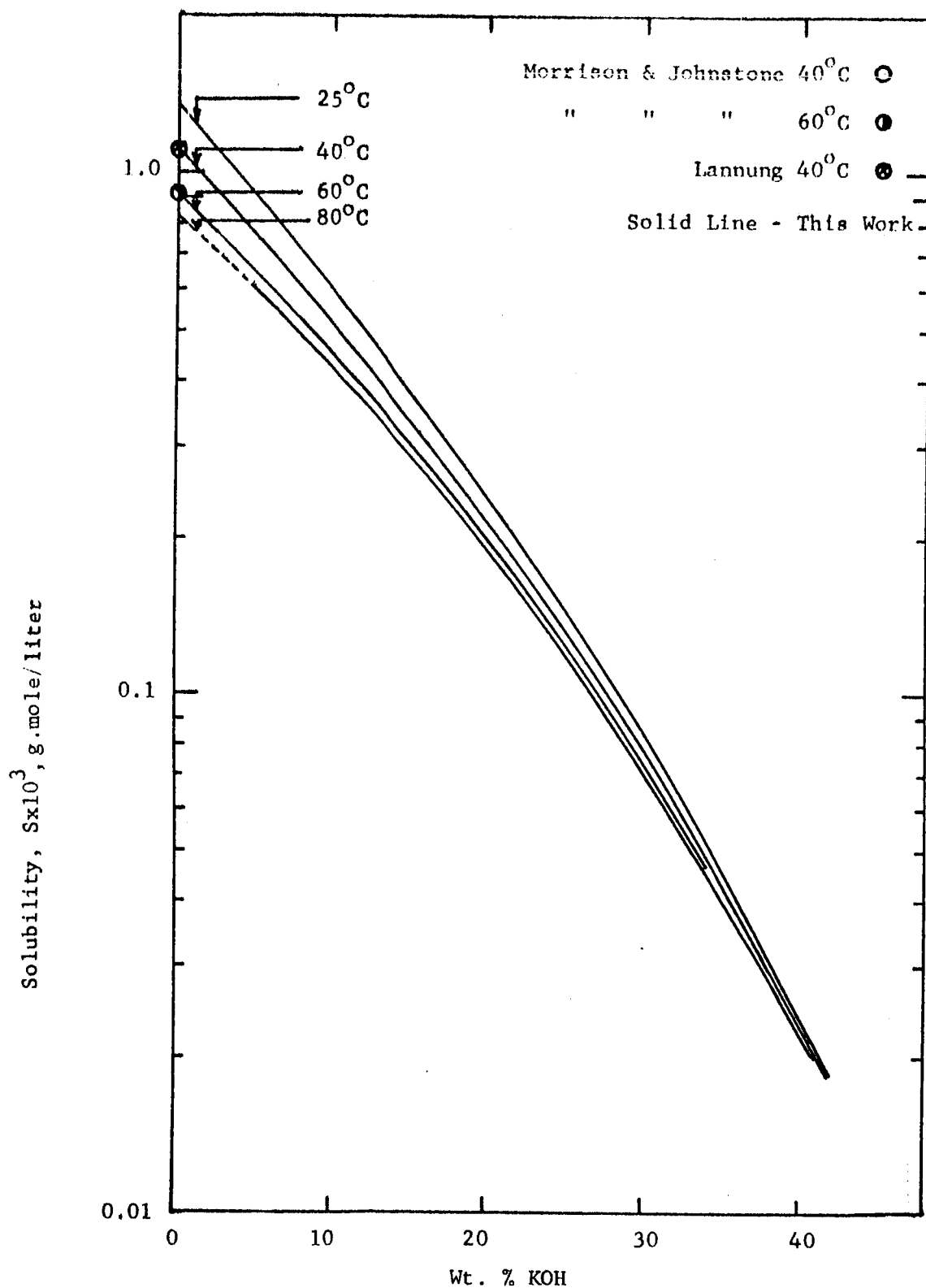


Figure 2.3 SOLUBILITY OF ARGON IN AQUEOUS POTASSIUM HYDROXIDE SOLUTIONS

The values reported here at 60°C are smaller than those reported in the Third Semi-Annual Report (8) by amounts up to about 8%. The differences may be explained in terms of the incomplete presaturation obtained in making the earlier measurements, as discussed above.

2.2.2 Solubility of Hydrogen

It may be seen from Figure 2.2 that at a temperature of 25°C, the data reported here are in fairly good agreement (within a few percent in most cases) with those of Geffcken (4) and Knaster and Apel'baum (7). However, at higher temperatures and concentration the disagreement is greater. The values reported by Ruetschi (8) at 30°C in his recent work are substantially lower than one would expect from earlier work.

2.2.3 Solubility of Argon

No data for the solubility of argon in aqueous potassium hydroxide solutions appear to be available in the open literature. However, a considerable amount of work on the solubility of this gas in water has been done. It can be seen from Figure 2.3 that the results reported here are in excellent agreement (within 1.5%) with those of Lannung (10) for the solubility of argon in water.

2.3 Discussion

The data reported here, as well as those of earlier investigators, show that the solubility of oxygen, hydrogen and argon decreases very rapidly with increase in potassium hydroxide concentration. Such a decrease of solubility of a neutral molecule as a result of the addition of an electrolyte is called the "salting out effect". It may be seen from Figures 2.1, 2.2 and 2.3 that this effect is less pronounced for hydrogen than for oxygen and

argon. Further, the degree of "salting out" is approximately the same for oxygen and argon.

It may be pointed out that no complete and reliable theory is available as yet which explains this type of effect. It is obvious, however, that any theory which attempts to explain "salting in" and "salting out" effects must consider the electrostatic as well as the dispersion forces between various ions and molecules. At present, an attempt is being made to develop a suitable theory to explain the solubility phenomena.

2.3.1 Partial Molal Heats of Solution

It may also be seen from the figures that the solubility of these gases changes with temperature. The change in solubility with temperature is more pronounced at lower temperatures than at higher ones. This can be easily and quantitatively seen by the calculation of partial molal heats of solution.

For a dilute solution of a gas in a liquid, the temperature dependence of the Henry's Law constant is given by the following thermodynamic expression:

$$\frac{\partial \ln K}{\partial T} = - \frac{(\bar{H}_1^o - h_1^g)}{RT^2} = - \frac{\Delta \bar{H}}{RT^2} \quad (2.3-1)$$

where $p_1 \simeq f_1 = Kx_1$

where p_1 , f_1 and x_1 are the partial pressure, fugacity and mole fraction of the solute gas.

The term \bar{H}_1^o is the partial molal enthalpy of the gas at infinite dilution and h_1^g is the molal enthalpy of the gas at pressure sufficiently low that the vapor phase behaves ideally. Then $(\bar{H}_1^o - h_1^g) = \Delta \bar{H}$ is the

molal heat of solution for an infinitely dilute solution. The above relation can be written in a more convenient form, as:

$$\frac{\partial \text{Log } K}{\partial \left(\frac{1}{T}\right)} = \frac{\bar{H}_i^o - h_i^g}{2.303R} = \frac{\Delta \bar{H}}{2.303R} \quad (2.3-2)$$

Thus, to obtain $\Delta \bar{H}$, the molal heat of solution, Log K was plotted against reciprocal absolute temperature. Figures 2.4, 2.5 and 2.6 show such plots for oxygen, hydrogen and argon, respectively. The calculated values of heats of solution are plotted in Figures 2.7, 2.8 and 2.9 which show the dependence of $\Delta \bar{H}$ on temperature for oxygen, hydrogen and argon, respectively. For hydrogen the curves corresponding to 20% and 30% KOH are almost indistinguishable. It is seen from these plots that the heat of solution is negative at lower potassium hydroxide concentrations and it becomes less negative as the potassium hydroxide concentration increases. Also, at lower temperatures the heat of solution is more negative. This indicates that the solubility changes rapidly at low temperatures and that the effect of temperature on the solubility is much less marked at higher potassium hydroxide concentrations.

2.3.2 Entropy of Solution

Hildebrand (11) derived an expression for the partial molal entropy of solution of gases in liquids which can be expressed as:

$$\bar{S}^o - S^g = R \left(\frac{\partial \ln a}{\partial \ln x} \right)_T \left(\frac{\partial \ln x}{\partial \ln T} \right)_P \quad (2.3-3)$$

where $\bar{S}^o - S^g = \Delta \bar{S}$ is the entropy change for a differential process per mole of the gas during solution. Since the solution is dilute, Henry's law can be assumed and then for a solubility process in which the gas

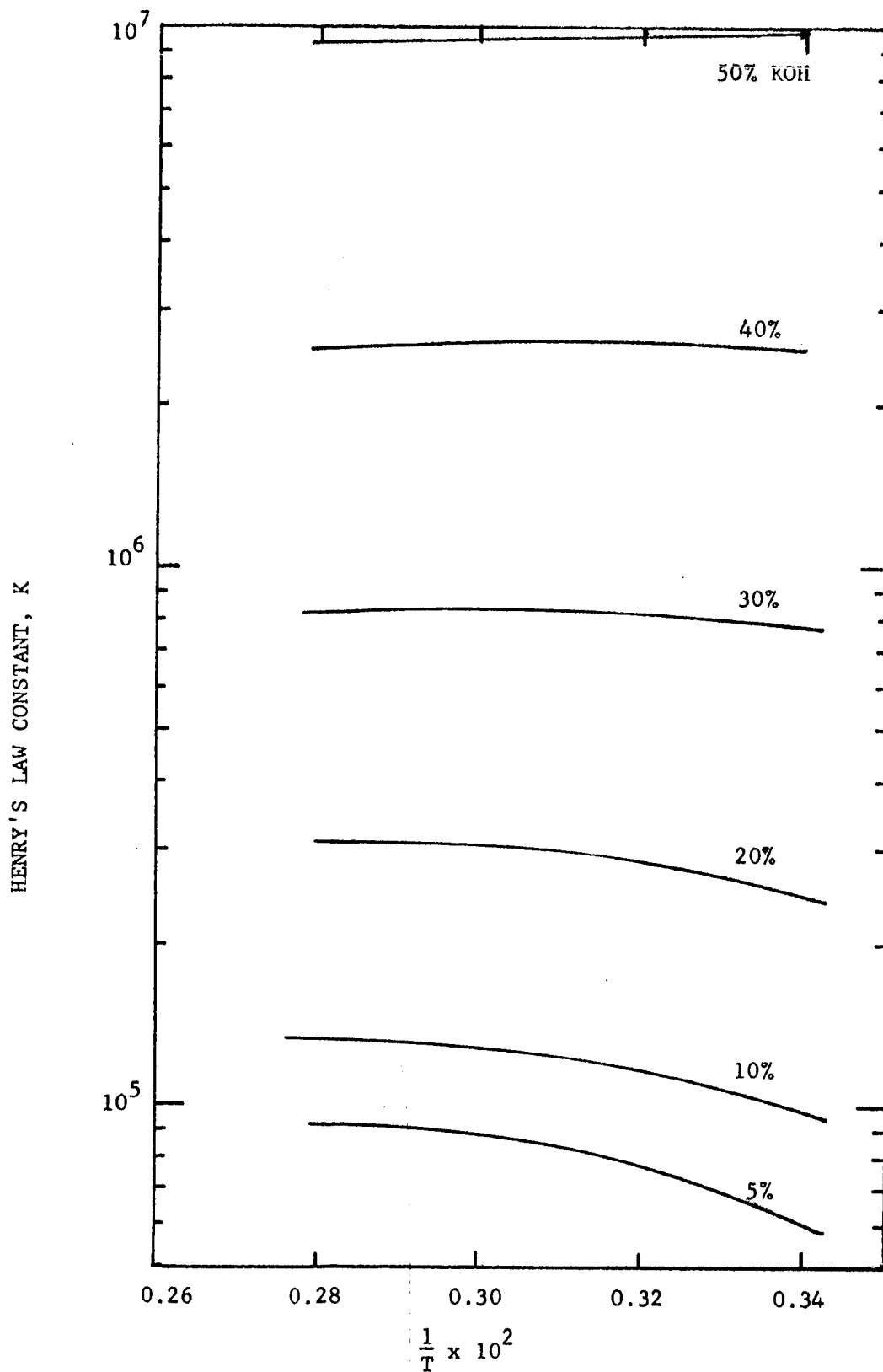


Figure 2.4 HENRY'S LAW CONSTANT FOR O_2 -AQUEOUS KOH SYSTEM

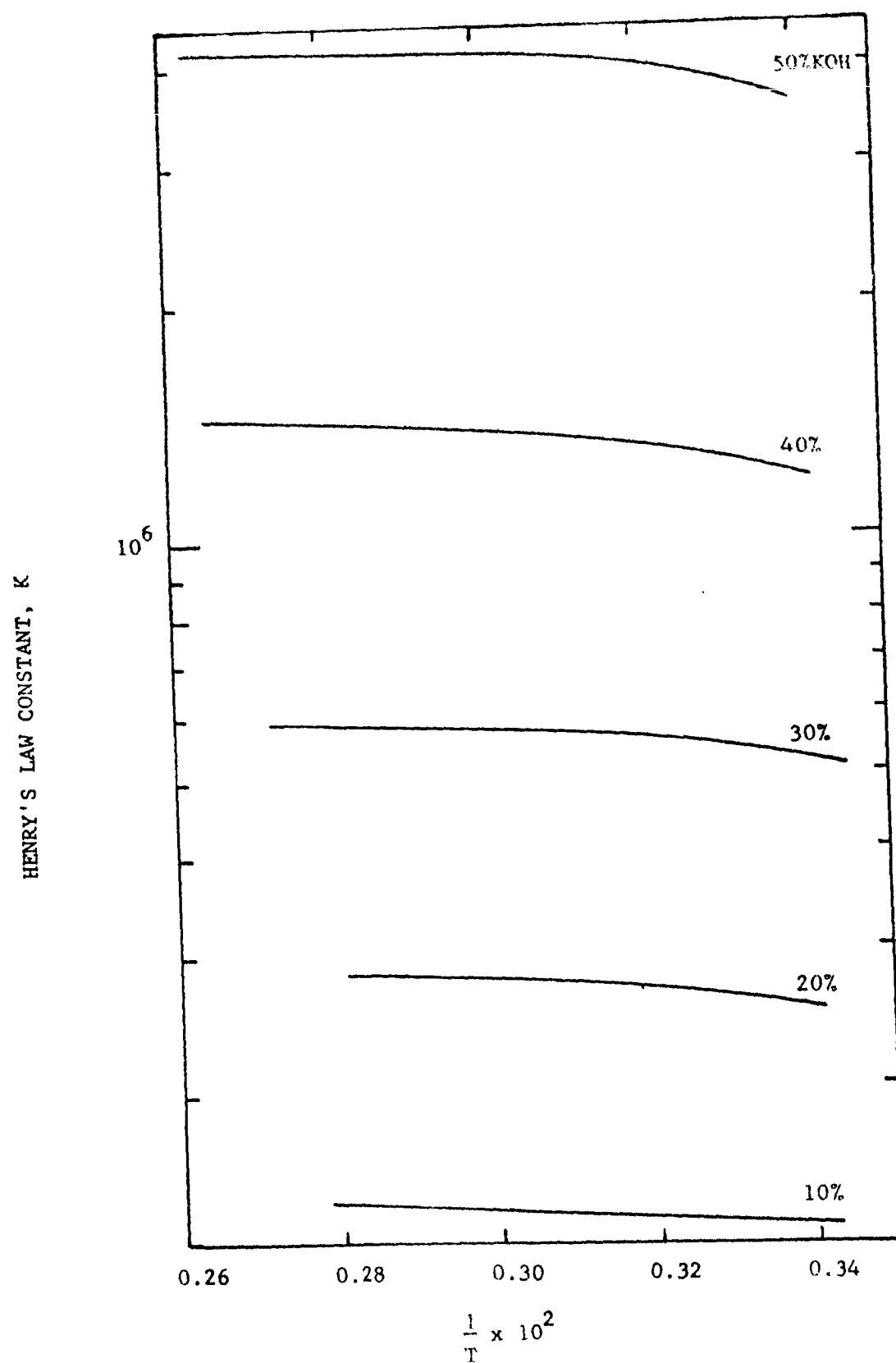


Figure 2.5 HENRY'S LAW CONSTANT FOR H_2 -AQUEOUS KOH SYSTEM

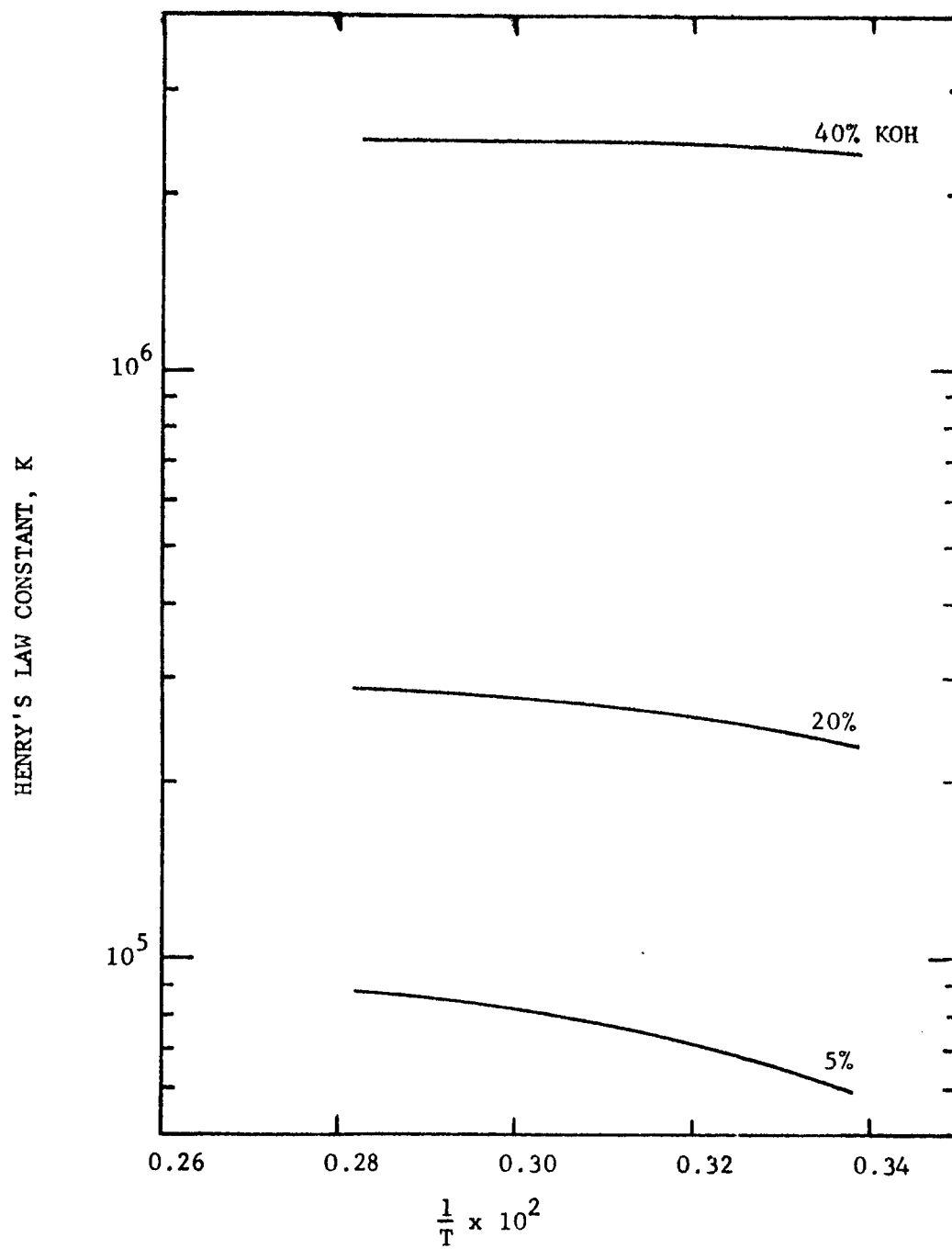


Figure 2.6 HENRY'S LAW CONSTANT FOR Ar-AQUEOUS KOH SYSTEM

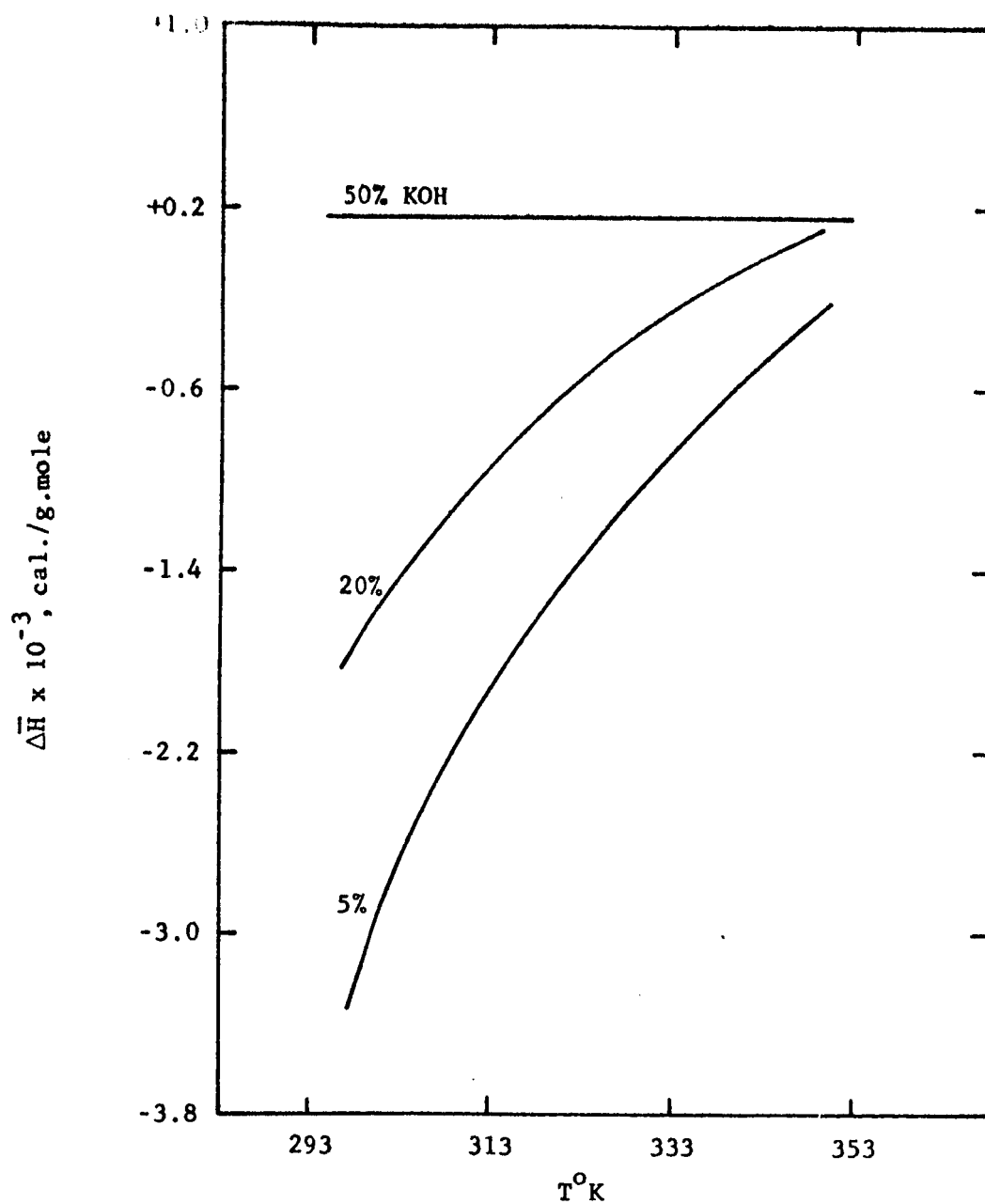


Figure 2.7 HEATS OF SOLUTION FOR O₂-AQUEOUS KOH SYSTEM

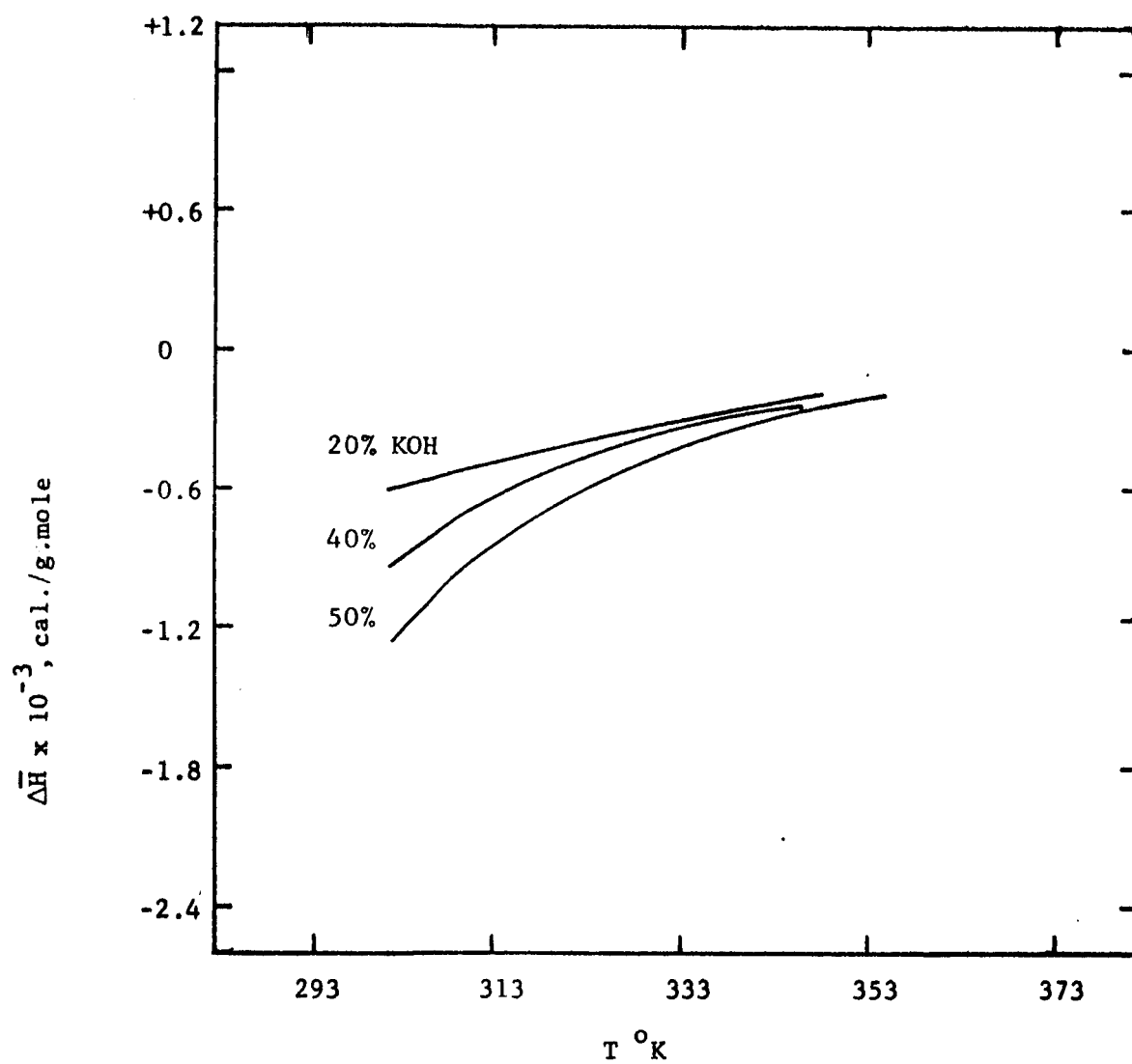


Figure 2.8 HEATS OF SOLUTION FOR H_2 -AQUEOUS KOH SYSTEM

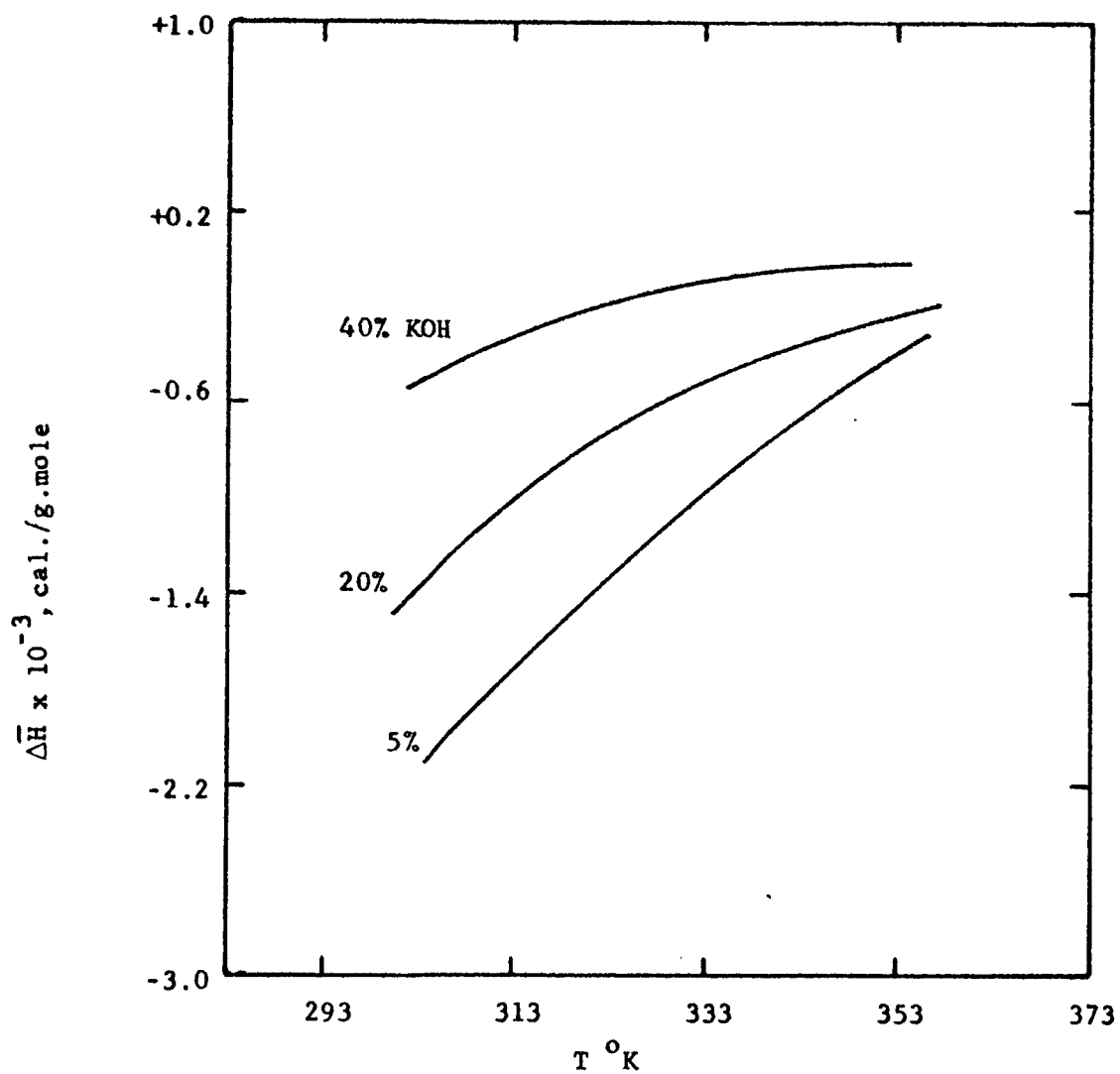


Figure 2.9 HEATS OF SOLUTION FOR Ar-AQUEOUS KOH SYSTEM

pressure is one atmosphere one can write

$$\frac{\partial \ln x}{\partial \ln T} = \frac{\partial \ln \frac{1}{K}}{\partial \ln T} = - \frac{\partial \text{Log } K}{\partial \text{Log } T} \quad (2.3-4)$$

Thus to get $\Delta \bar{S}$, the Henry's law constant was plotted against temperature on logarithmic co-ordinates. Entropies of solution were then found from the slope of the plot.

The calculated entropies of solution for oxygen and argon have been plotted against temperature in Figures 2.10 and 2.12. It may be noticed from these plots that the entropy change becomes less negative as temperature or potassium hydroxide concentration increases. The entropy of solution for hydrogen is relatively constant with respect to temperature. However, it becomes less negative as the potassium-hydroxide concentration increases. Figure 2.11 shows such variations.

2.3.3 Energy of Solution

It has been shown (12,13) that the energy of solution of a gas molecule in a solvent is an important variable for correlating and predicting gas solubilities. Elley (14) divided the energy of solution of a gas molecule into the energy of cavity formation and energy of introduction of the gas molecules into the cavity. He showed that for a given gas, the energy of cavity formation varied widely with the kind of solvent, and that various gases had much the same value of energy of introduction of the gas molecule into the solvent.

The energy of solution is given by the following relation:

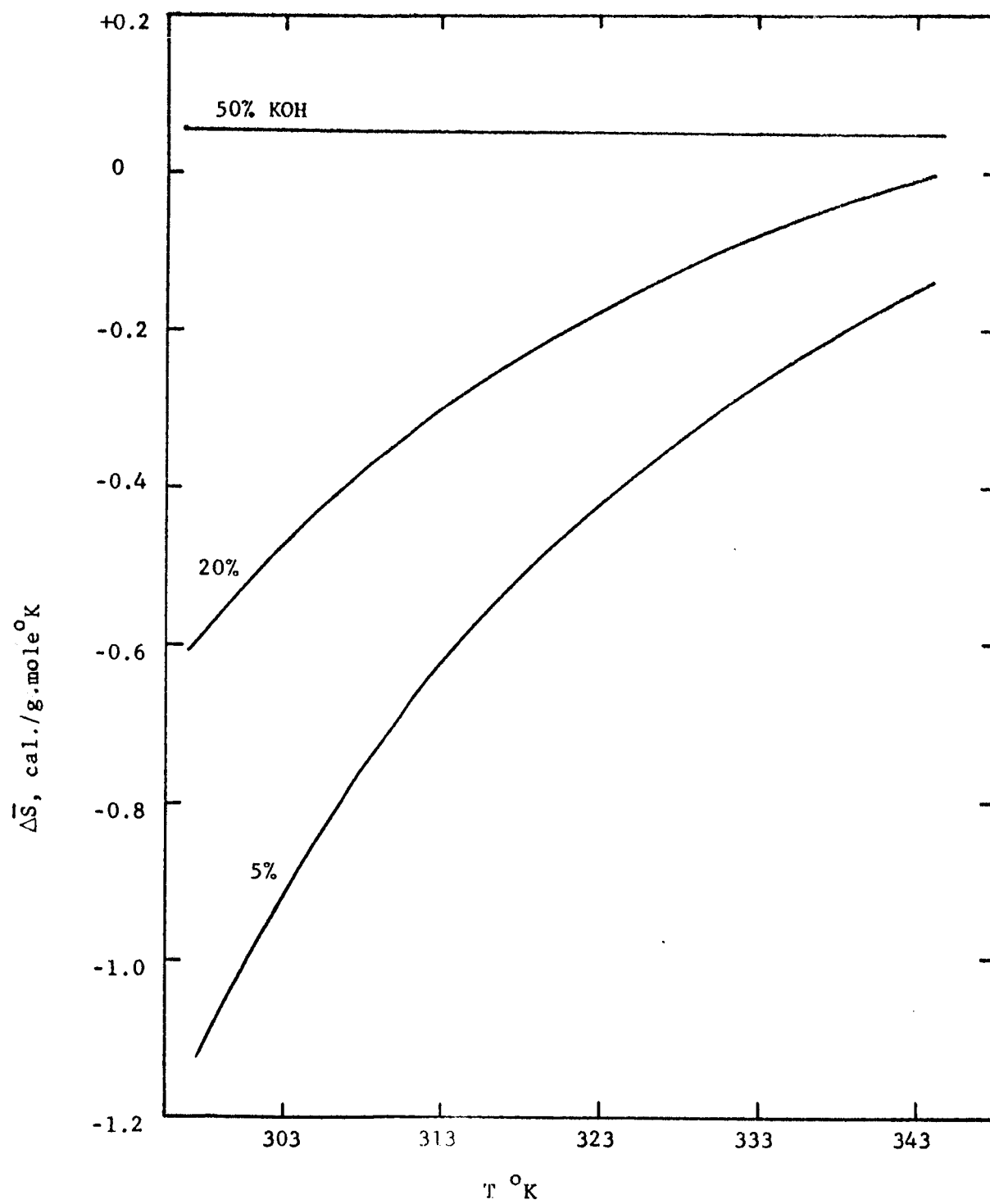


Figure 2.10 ENTROPIES OF SOLUTION FOR O₂-AQUEOUS KOH SYSTEM

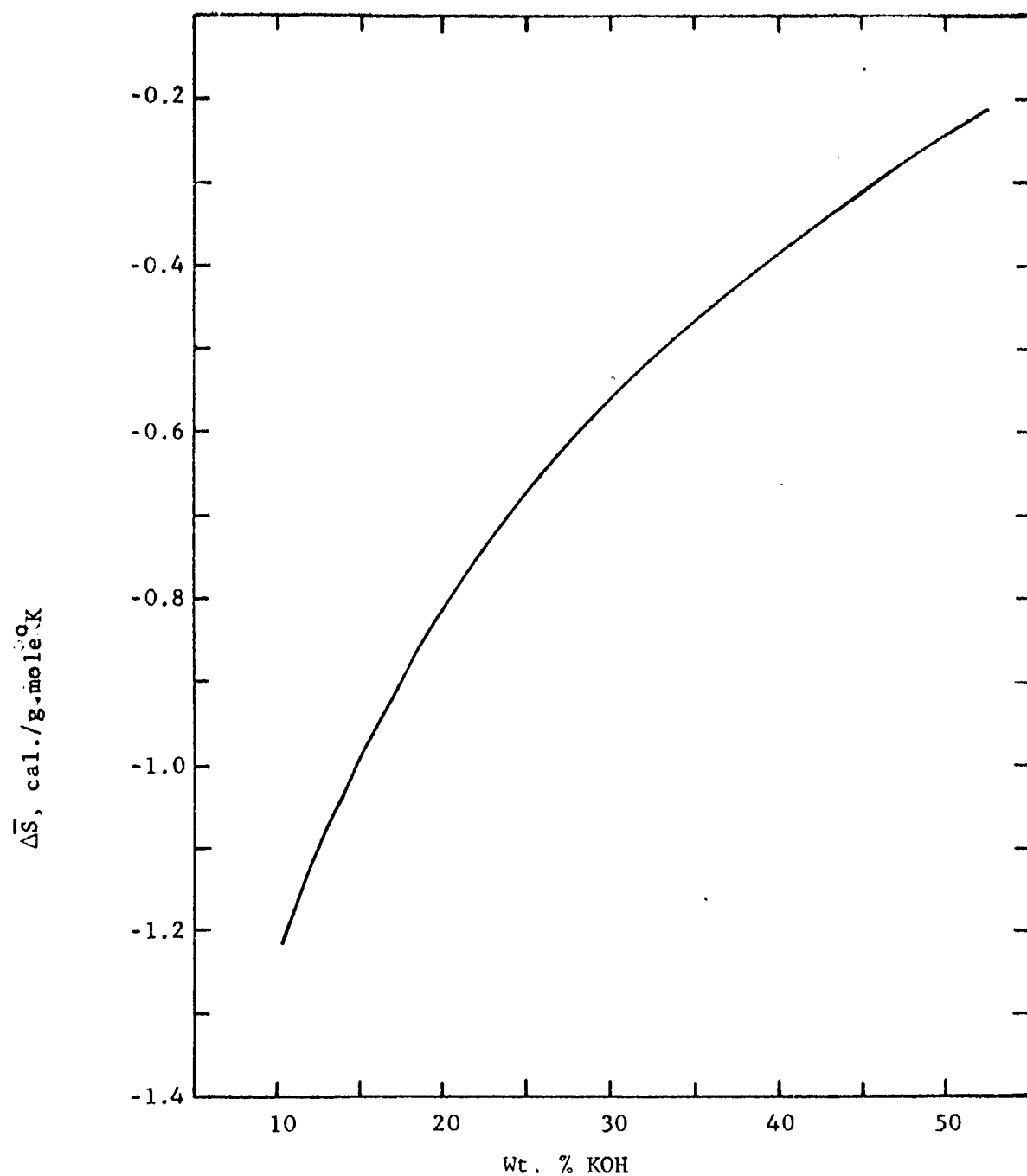


Figure 2.11 ENTROPIES OF SOLUTION FOR H_2 -AQUEOUS KOH SYSTEM

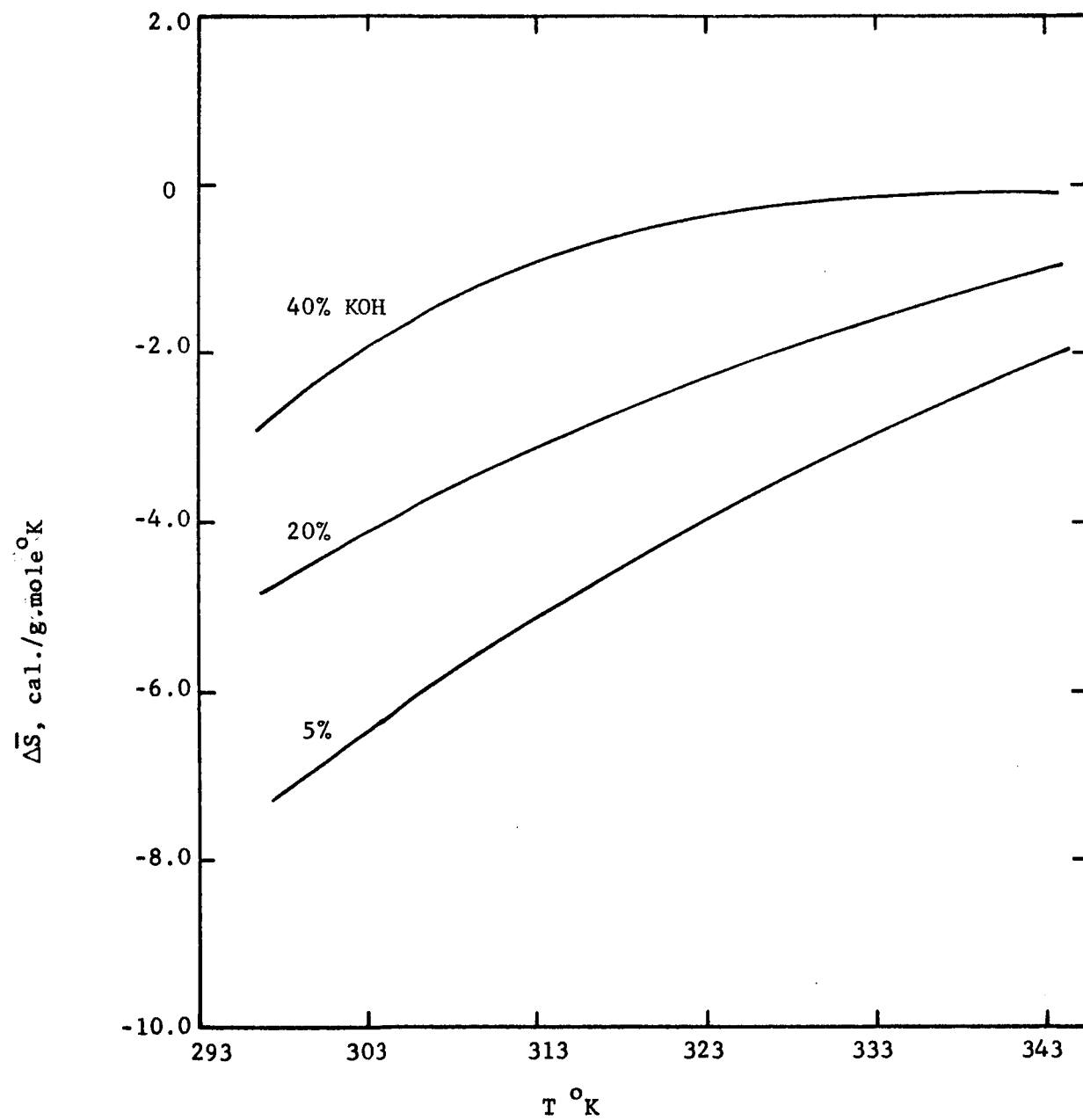


Figure 2.12 ENTROPIES OF SOLUTION FOR Ar-AQUEOUS KOH SYSTEM

$$\Delta \bar{H} = \bar{H}_i^o - h_i^g = \left(\bar{E}_i^o + p\bar{V}_i^o \right) - \left(E_i^g + pV_i^g \right) \quad (2.3-5)$$

$$= \Delta \bar{E} + p \left(\bar{V}_i^o - V_i^g \right)$$

$$\simeq \Delta \bar{E} - pV_i^g \quad (2.3-6)$$

since \bar{V}_i^o is much less than V_i^g

The gas pressure encountered is low, so that we can assume the ideal gas law. Thus

$$\Delta \bar{E} = \Delta \bar{H} + RT \quad (2.3-7)$$

Calculated values of $\Delta \bar{E}$ are plotted in Figures 2.13, 2.14 and 2.15. It is seen that energies of solution are negative and become less negative as the potassium hydroxide concentration or the temperature is increased.

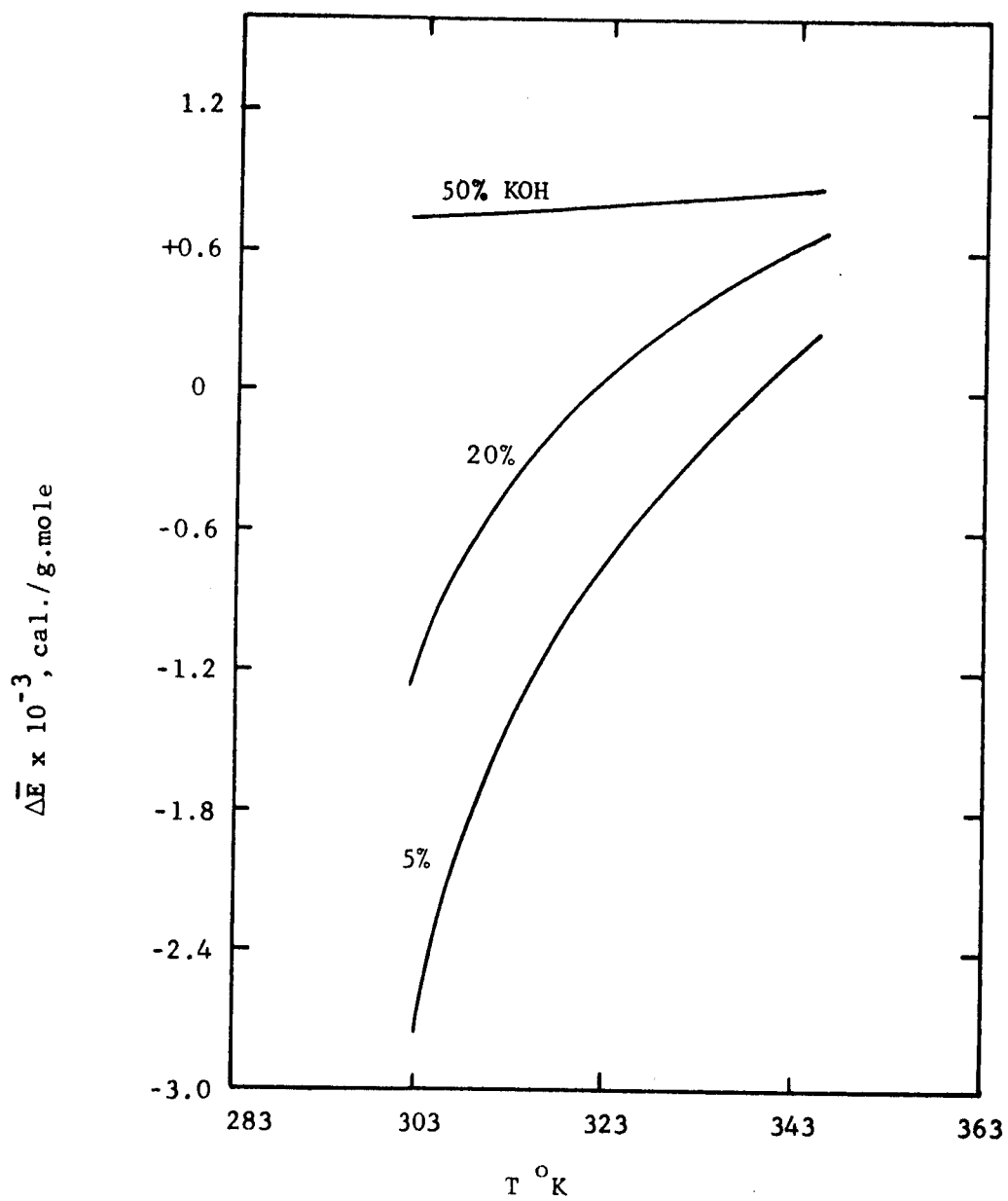


Figure 2.13 ENERGIES OF SOLUTION FOR \dot{O}_2 -AQUEOUS KOH SYSTEM

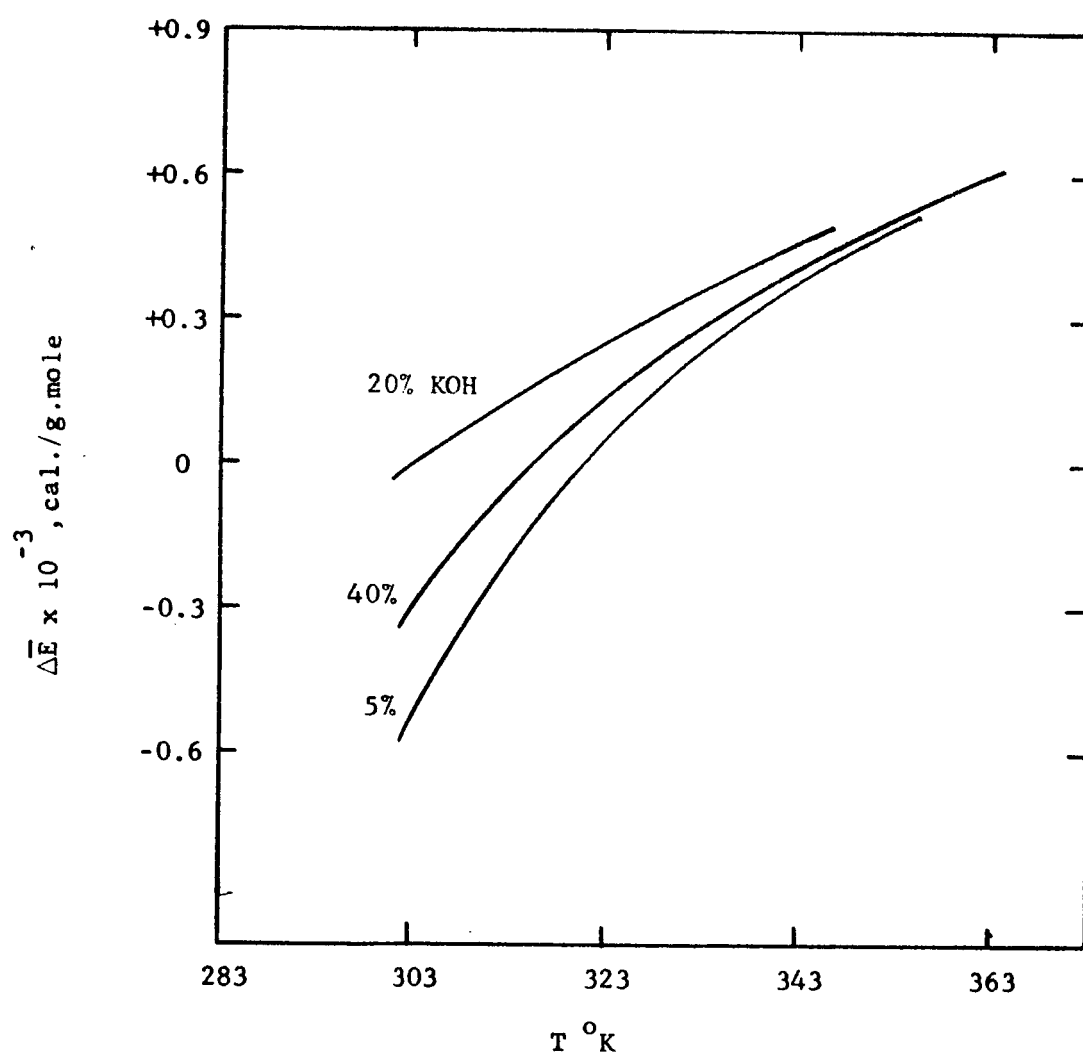


Figure 2.14 ENERGIES OF SOLUTION FOR H_2 -AQUEOUS KOH SYSTEM

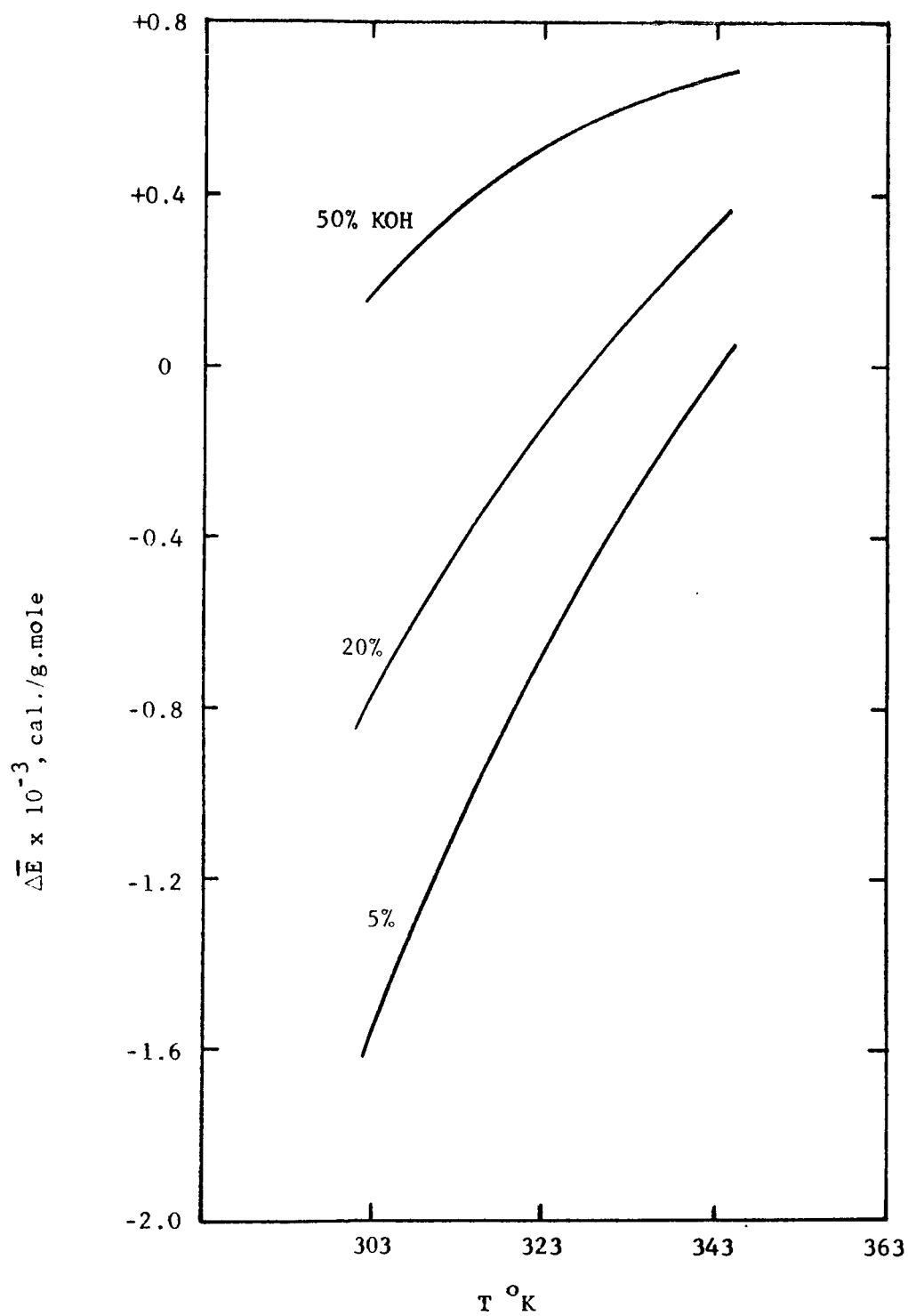


Figure 2.15 ENERGIES OF SOLUTION FOR Ar-AQUEOUS KOH SYSTEM

3. The Diffusivity of Oxygen and Hydrogen in KOH Solutions - M. K. Tham

Because of the slowness of diffusion in liquids, accurate measurements of diffusion coefficients are often difficult and time consuming. In the case of oxygen diffusing in KOH solutions, the very low concentration of dissolved gas presents additional analysis difficulties. Several methods of measuring diffusivity in concentrated KOH solutions were considered; these included those employing a diaphragm cell and those based on electrochemical reaction at an electrode.

Detailed consideration of the steady-state diaphragm cell method discussed in a previous report (3) suggested that, in view of the very low solubility of the dissolved gases at high KOH concentrations (see Section 2), severe difficulties would arise in measuring the low concentrations of diffused gas. The unsteady-state diaphragm cell method also appeared to be unsuitable for similar reasons. Low concentrations of dissolved gases appeared to be somewhat less of a limitation on electrochemical methods, and a number of these were considered. Polarography with the dropping mercury electrode may be used for diffusing O_2 , but is not applicable to diffusion of H_2 (15). The rotating disc electrode presents problems at high KOH concentrations where it appears that activation polarization becomes appreciable, and the process may not be diffusion controlling (5). The method adopted for these measurements was the stagnant diffusion cell method which is described below. This method is simple, and appears to be applicable to measurements of the diffusivity of both oxygen and hydrogen.

3.1 Experimental

3.1.1 Theory

The stagnant diffusion cell is shown schematically in Figure 3.1. A capillary which forms the diffusion path with an electrode at one end is immersed in the electrolytic solution saturated with the diffusing substance. (Contact of the electrode with the solution is made through the capillary only.) When a DC voltage is applied to the system, the reducible (or oxidizable) substance will react at the electrode, where a concentration gradient will be developed and diffusion will take place. The flux of the reducible species will increase with an increase in applied voltage, until a certain voltage is reached at which the supply of the diffusing reactant substance cannot keep up with the consumption of the species; at this voltage the concentration at the electrode becomes zero, and diffusion is said to be controlling.

When such a potential is applied to the cell, the equation of continuity for the diffusing species with no convection mass transfer is given by

$$\frac{\partial C}{\partial t} = D \frac{\partial^2 C}{\partial x^2} \quad (3.1-1)$$

where C = the concentration at any distance from the electrode x , and time t ,

D = the diffusivity

with the following conditions

Initial Condition: $C = C_0$ when $t = 0$, for all x

Boundary Condition: $C = 0$ when $x = 0$, for $t > 0$

Solving equation (3.1-1) with the I.C. and B.C. gives

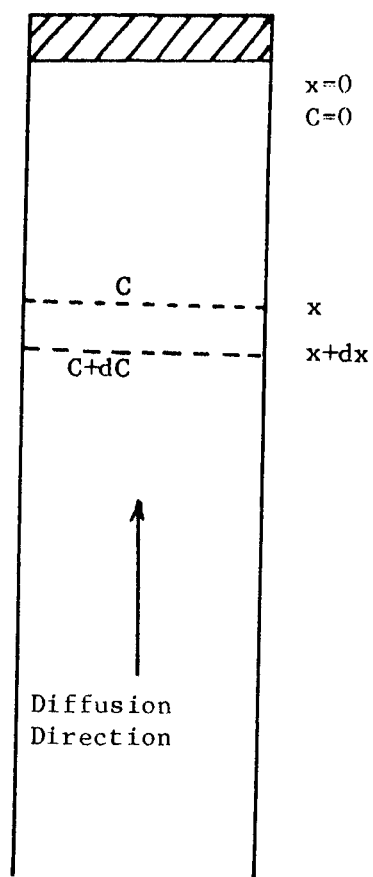


Figure 3.1 Schematic Diagram of Linear Diffusion in a Stagnant Cell

$$C = \frac{\partial C_o}{\sqrt{\pi}} \int_0^{\frac{x}{2\sqrt{Dt}}} e^{-y^2} dy \quad (3.1-2)$$

where y is a dummy variable.

The limiting current, being proportional to the flux of the species, is given by

$$I_{lim} = nFA D \left(\frac{\partial C}{\partial x} \right)_{x=0,t} \quad (3.1-3)$$

where n = no. of Faradays required per mole of electrode reaction

F = Faraday

A = area of diffusion path perpendicular to the direction of diffusion

$$\left(\frac{\partial C}{\partial x} \right)_{x=0} = \text{concentration gradient at } x=0$$

However, from Equation (3.1-2) we see that

$$\left(\frac{\partial C}{\partial x} \right)_{x=0} = \frac{C_o}{\sqrt{\pi Dt}}$$

and this lead to

$$I_{lim} = nFC_o A \sqrt{\frac{D}{\pi t}} \quad (3.1-4)$$

Solving Equation (3.1-4) for D we get

$$D = \pi T \left(\frac{I_{lim}}{nFC_o A} \right)^2 \quad (3.1-5)$$

3.1.2 Procedure

The simple linear diffusion cell as described by Kolthoff and Lingane (15) was used. It consisted of a platinum disc cemented between two glass capillaries with a pore diameter of 2.4 mm, and 1.5 inches in length. The silver counter electrode, placed well away from the capillary

mouth used, had an area of 20 cm^2 . A Sargent Polarograph, Model XV was used for both applied voltage and current measurement.

Determination of the capillary area was made by measuring the diffusion current of 0.0005 M Potassium Ferricyanide solution in 0.1 N KCl solution. Accurate diffusivity for this system have been reported previously by von Stackelberg, et al. (16).

The KOH solution was saturated with oxygen at a particular temperature by bubbling through the solution for 30 minutes. Oxygen was again bubbled through the solution for 5 minutes before each repetition of measurement.

The electrode was cleaned by cathodic evolution of hydrogen and the capillary was then filled with fresh solution by injecting with a syringe, 5 to 10 minutes was allowed for the system to reach equilibrium before a voltage of -0.5 volt (with reference to a saturated calomel electrode) was applied. This voltage was chosen as being approximately in the middle of the first plateau of the voltage-current curve for oxygen reduction; this first plateau corresponds to the reduction of oxygen to peroxide. The current was recorded as a function of time.

In all experiments diffusion was in the upward direction. When the direction of diffusion was downward, the measured current was very high and at times tended to be unstable. This was attributed to density gradients which formed during diffusion. In view of the fact that the concentrations of KOH and water are very large compared to that of the dissolved gas, transport of OH^- ions and water would not appear likely to be a limiting factor. Strong evidence that transport of dissolved oxygen was the only diffusive flux that affected the measured

current was provided by the fact that the limiting current varied as $t^{-\frac{1}{2}}$, as required by Equation (3.1-4).

3.2 Results and Discussion

The results of the diffusion measurements at 25°C are plotted in Figure 3.2, together with those reported earlier by Gubbins and Walker (17), and Tobias et al. (5) and are tabulated in Table 3.2. The results are slightly lower than those reported by the earlier workers at high concentration. No measurements at higher concentrations were made because of the low limiting currents. Other means for the measurement of these small currents will be explored, one of which is to increase the capillary size.

The accuracy of the determination of concentration is estimated to be $\pm 0.1\%$. Temperature is controlled to 0.2°C. The deviations given are standard deviation from the arithmetic mean.

For electrolytic solutions, transport properties, such as the diffusivity or viscosity, appear to be an exponential function of the species fraction of the electrolyte - defined as $\frac{x}{1-x+(\nu^+ + \nu^-)x}$ (where x is the mole fraction of KOH and ν^+ is the valence of the ions). The diffusivity values reported here, which are plotted on semi-log paper in Figure 3.3, do give a good straight line, indicating that the predicted relationship holds for the temperature and concentration range where data are available.

The value of diffusion coefficient when extrapolated to 0% KOH gives a value $1.91 \times 10^{-5} \text{ cm}^2/\text{sec.}$, in good agreement with that reported in the literature.

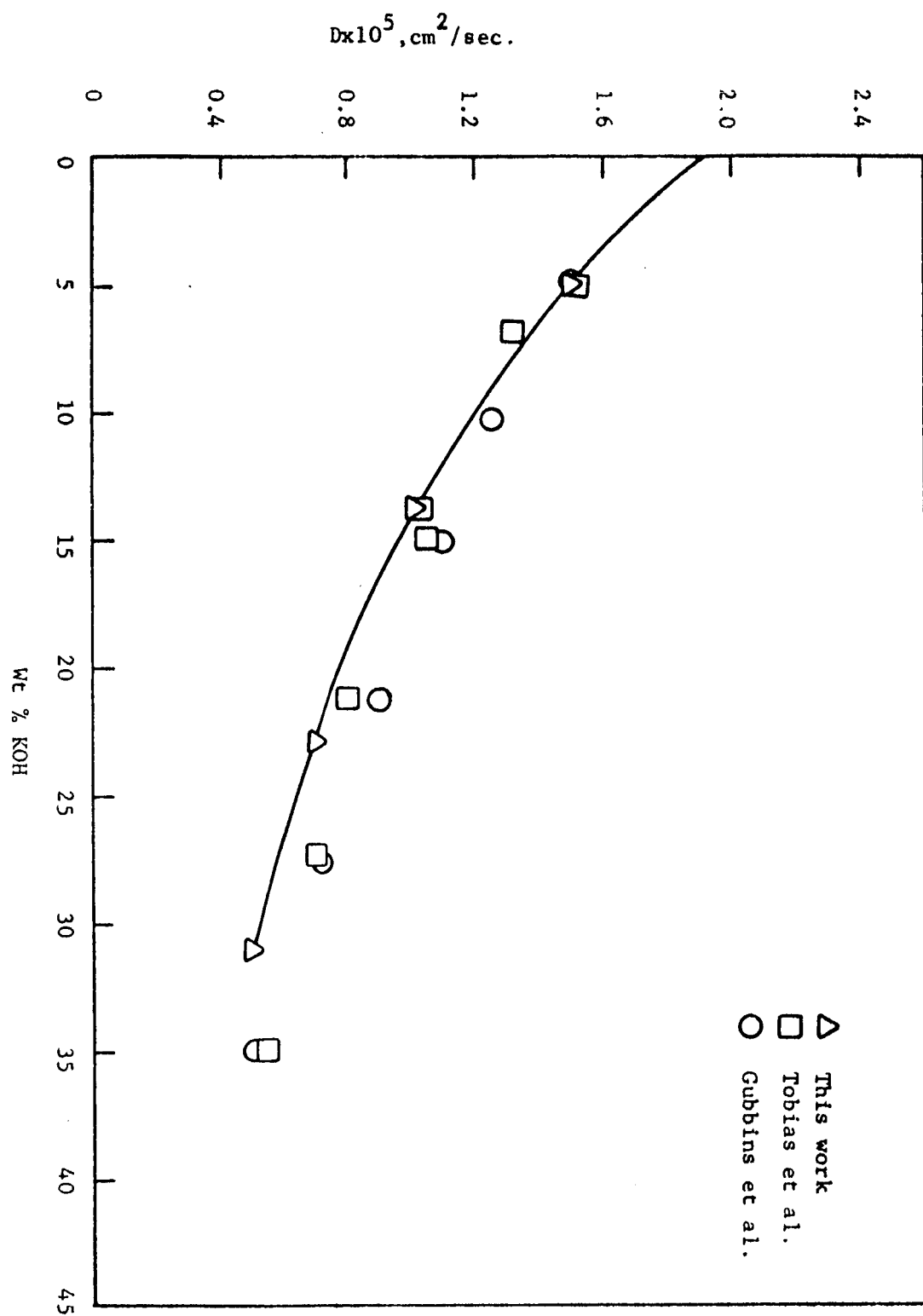


Figure 3.2 Diffusivity of Oxygen in Potassium Hydroxide Solutions at 25°C

Table 3.2

Diffusion Coefficient of O_2 in KOH Solutions at $25^\circ C$

Concentration (Wt % KOH)	$D \times 10^5, \text{ cm.}^2/\text{sec.}$
5	1.481 ± 0.021
13.5	1.002 ± 0.01
23	0.683 ± 0.014
31.5	0.501 ± 0.014

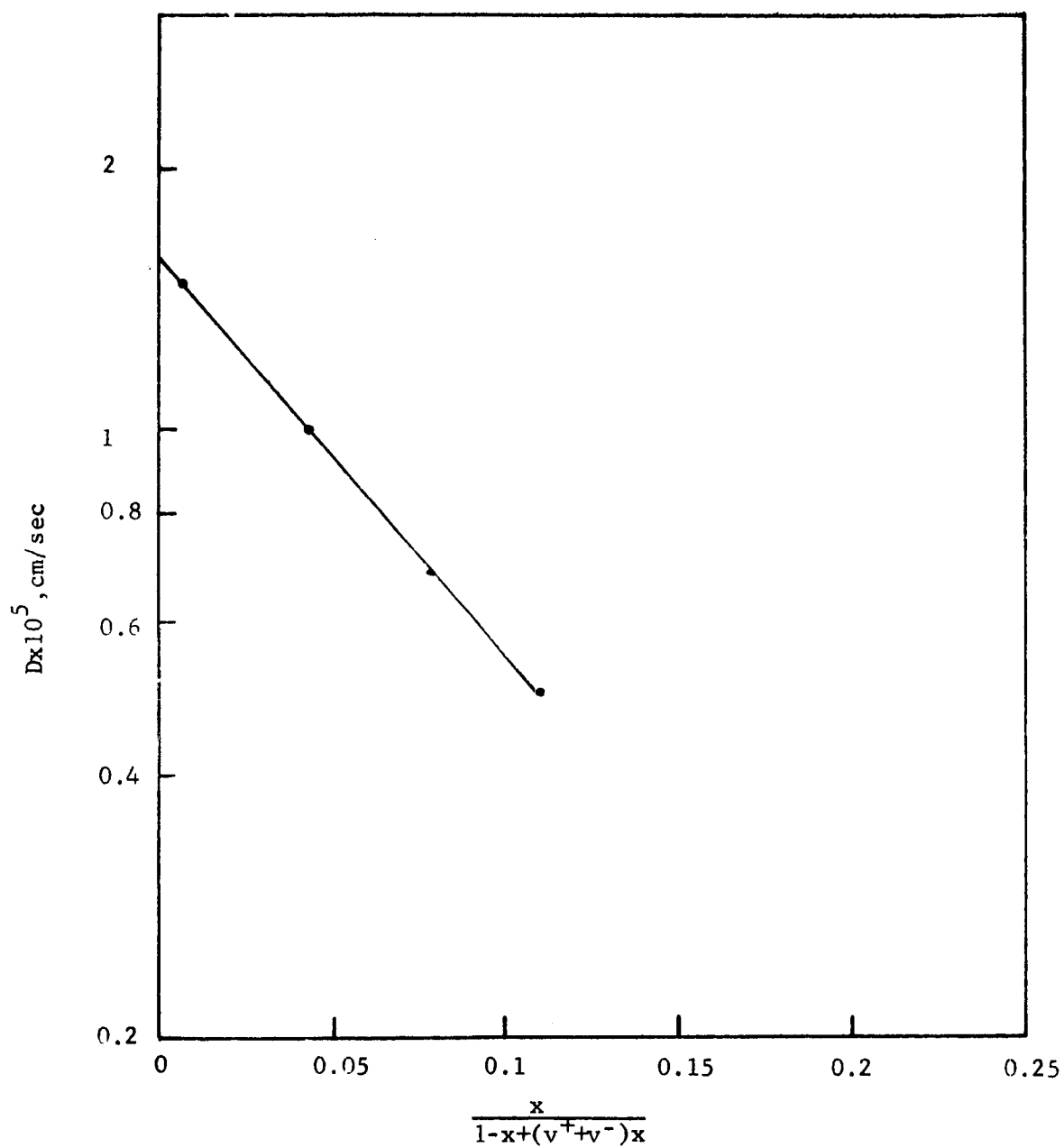


Figure 3.3 Relationship of Diffusivity of Oxygen to Species Fraction of Potassium Hydroxide

As can be seen from the data, the diffusion coefficient of O_2 in KOH drops rapidly with increase in KOH concentration. The value of the diffusivity at 31.6 wt % KOH is only about 30% of that in pure water.

It is interesting to note that the data reported by Gubbins and Walker, which were obtained by a polarographic method are about 10% higher than those reported by Tobias. Gubbins and Walker took the constant A in the modified Ilkovic equation,

$$i_d = 607nD^{1/2} C_m^{2/3} t^{1/6} \left(1 + \frac{AD^{1/2} t^{1/6}}{m^{1/3}} \right)$$

as 31.5, as recommended by Meites and Meites (18). If a value of A = 39 is used as recommended by Lingane and Loveridge (19) the agreement of the two sets of data is very good, which emphasizes the importance of the choice of the value for the constant A.

Diffusion coefficients of H_2 in KOH solutions at 30°C were measured by Rüetschi using a rotating disk electrode (9), and are plotted in Figure 3.4.

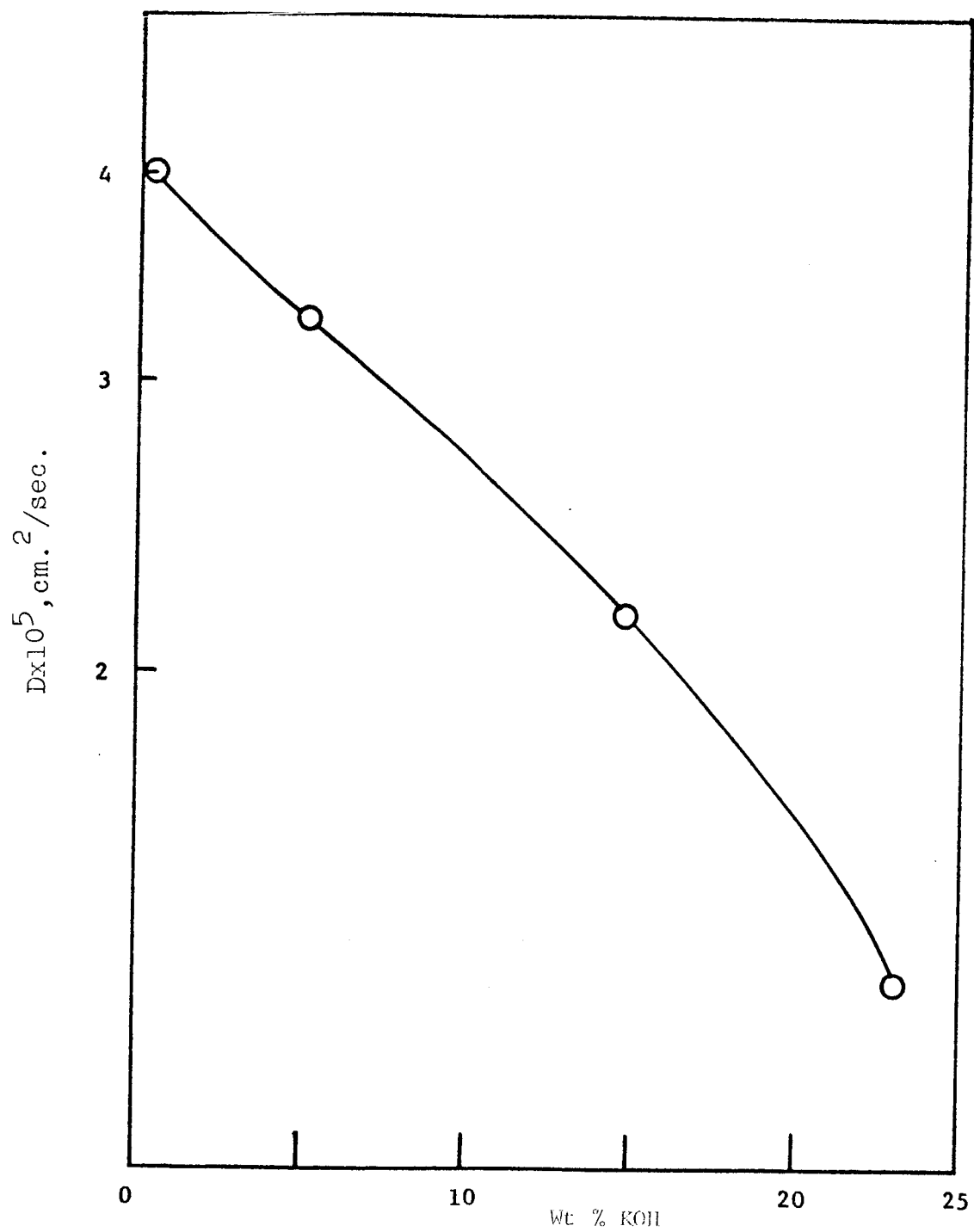


Figure 3.4 Diffusivity of Hydrogen in Potassium Hydroxide Solutions at 25°C

4. Diffusion of Water in Potassium Hydroxide Solutions - R. N. Bhatia

Measurements have been made of the integral mutual diffusivity for aqueous potassium hydroxide solutions for the entire concentration range, and for temperatures in the range 25-75°C. The experimental apparatus and procedure, and the method of calculating differential diffusion coefficients from experimental integral data, were described in detail in the Third Semi-Annual Report (20). The relationship between the integral and differential diffusion coefficients is given by

$$\bar{D} = \frac{1}{t} \int_0^t dt \left(\frac{1}{C' - C''} \right) \int_{C''}^{C'} D dC \quad (4.1-1)$$

Details of the method for calculating D from \bar{D} data may be found in Appendix 2.

4.1 Results

Tables 4.1 and 4.2 show the integral and differential diffusion coefficient values respectively. In Table 4.1, the terms c_1 and c_2 are the initial KOH concentrations in the lower and upper cell compartments in units (g.mole.l.⁻¹); c_2 had the value zero in all experiments. The differential values shown in Table 4.2 are the values normally used, and are diffusion coefficients on the volume-fixed reference frame, defined by

$$J = - D \frac{\partial c}{\partial x} \quad (4.1-1)$$

where J is the flux of diffusing material referred to the (moving) center of volume. This is the reference frame most commonly used, and has the advantage that the diffusion coefficients of the two components are equal.

TABLE 4.1
INTEGRAL DIFFUSION COEFFICIENTS OF AQUEOUS KOH SOLUTIONS
 $(c_2=0)$; \bar{D} in $\text{cm.}^2 \text{ sec.}^{-1}$

25°C		45°C		65°C		75°C	
c_1	$\bar{D} \times 10^5$	c_1	$\bar{D} \times 10^5$	c_1	$\bar{D} \times 10^5$	c_1	$\bar{D} \times 10^5$
0.103	2.70	0.103	3.87	0.103	5.89	0.690	6.80
0.103	2.662	0.103	3.92	0.103	5.79	0.690	6.84
0.103	2.70	0.477	3.86	0.477	5.68	0.912	7.28
0.477	2.67	0.912	3.90	0.912	5.84	0.912	7.23
0.477	2.67	0.912	3.87	0.912	5.89	1.906	7.64
1.050	2.74	1.906	4.14	1.906	6.07	1.906	7.54
1.050	2.70	1.906	4.10	1.906	6.10	4.156	8.36
2.080	2.91	4.156	4.65	4.156	6.75	4.156	8.29
2.080	2.89	4.156	4.68	4.156	6.78	7.008	8.49
4.555	3.19	7.008	5.08	7.008	7.02	7.008	8.46
4.555	3.18	7.008	5.01	9.846	7.12	9.846	8.69
7.668	3.46	9.846	5.11	9.846	7.13	9.846	8.60
7.668	3.50	9.846	5.11	12.616	7.25	12.616	8.74
7.668	3.52	11.742	5.19	12.616	7.27	12.616	8.87
10.667	3.55	12.616	5.24				
10.667	3.58	12.616	5.21				
10.667	3.60						
13.720	3.62						
13.720	3.66						

TABLE 4.2

DIFFERENTIAL DIFFUSION COEFFICIENTS OF AQUEOUS KOH SOLUTIONSThe reported values are $D \times 10^5$ ($\text{cm}^2 \text{sec}^{-1}$)

<u>KOH. Concn.</u>	<u>25°C</u>	<u>45°C</u>	<u>65°C</u>	<u>75°C</u>
0.040	2.70	3.89	5.76	6.70
0.160	2.66	3.83	5.67	6.89
0.360	2.67	3.86	5.73	6.94
0.640	2.75	4.05	5.96	7.29
1.000	2.87	4.15	6.22	7.72
1.440	3.02	4.36	6.49	8.11
1.960	3.15	4.61	6.74	8.45
2.560	3.30	4.85	6.91	8.64
4.000	3.56	5.21	7.17	8.98
5.760	3.75	5.29	7.30	8.89
7.840	3.78	5.26	7.30	8.74
9.925		5.15		
9.986		5.19		
10.240	3.66		7.27	8.80
12.250	3.66		7.16	
12.960				8.79

The cells were calibrated using both KCl and HCl solutions, for which accurate diffusion coefficient values are already available. Good agreement was obtained by the two methods. Measured cell constants were reproducible to within $\pm 0.7\%$. Calibrations were performed at frequent intervals to check against possible changes in the cell constant with time, but no detectable change was found. Chang and Wilke (21) have shown that changes in cell calibration constant with temperature are negligible.

The accuracy of the reported differential diffusivity data is estimated to be approximately $\pm 3\%$. This figure was arrived at by considering errors involved in operating the cells, in determining concentrations, cell calibration constant and time, and in the procedure used to calculate differential diffusivities from the experimental integral values.

4.2 Theory

At present there appears to be no satisfactory theory that may be used to predict mutual diffusion coefficients in concentrated electrolyte solutions. The Onsager-Fuoss theory (22) provides a rigorous approach that yields quantitatively correct values at concentrations up to about 0.01 molar, but attempts to extend its use to higher concentrations have been unsuccessful. However, in fuel cell (and most other) applications, concentrations much above this value are of interest. A theory based on a simple model for diffusion in concentrated electrolytes is presented below. The theory is a modification of Eyring and absolute reaction rate theory (23).

The equation obtained by Eyring for the mutual diffusion coefficient in a binary solution is

$$D = k_d \lambda^2 \exp \left(- \Delta G_o^* / RT \right) \left[\frac{\partial \ln a_A}{\partial \ln N_A} \right]_{T,p} \quad (4.2-1)$$

where k_d = constant

λ = jump constant

ΔG_o^* = free energy of activation per molecule

T = temperature

a_A = activity of component A (water)

N_A = mole fraction of A

The term $(\partial \ln a_A / \partial \ln N_A)$ is a thermodynamic nonideality term. We may define D^{id} by,

$$D^{id} = \frac{D}{\left(\frac{\partial \ln a_A}{\partial \ln N_A} \right)} = k_d \lambda^2 \exp(-\Delta G_o^* / RT) \quad (4.2-2)$$

so that D^{id} is a purely kinetic term, the thermodynamic factor having been removed.

The following derivation is similar to that of Podolsky (24) for viscosity of electrolytes. The value of D at infinite dilution (D^0) may be accurately predicted from the Nernst relation.

$$D^0 = \frac{RT(\nu_1 + \nu_2)}{F^2 \nu_1 |z_1|} \left[\frac{\lambda_1^0 \lambda_2^0}{\lambda_1^0 + \lambda_2^0} \right] \quad (4.2-3)$$

where $\nu_1 \nu_2$ = number of moles of ions 1 and 2 per mole of electrolyte

z_1 = charge for ion 1

F = Faraday

λ_1^0, λ_2^0 = experimentally measured limiting equivalent ionic conductances.

On increasing the electrolyte concentration, the ions are assumed to perturb ΔG_o^* from its original value, but λ is assumed to be relatively unaffected (this assumption has been shown a good approximation by Podolsky). Since the diffusion coefficients for water and KOH are equal on the volume frame, we shall confine our attention to the diffusion of water molecules. In addition we shall assume that the molecules and ions are randomly mixed; that is, the probability that a particle of species i is in a particular volume element is independent of the species of neighboring molecules. This assumption is known to be good for organic liquid mixtures (25).

Consider a water molecule interacting with n surrounding water molecules or ions. If C is the concentration of electrolyte in g.mole/liter and if one molecule of the electrolyte gives in solution ν_1 moles of ions of type 1 and ν_2 moles of ions of type 2, the number of i ions interacting with the central water molecule is

$$\frac{18 C n \nu_i}{(1000d - CM) + 18C(\nu_1 + \nu_2)}$$

where d is density and M is molecular weight. An ion of type i in the nearest neighbor ring is assumed to perturb the activation free energy by an amount δ_i per mole to $\Delta G^* + \delta_i$, where ΔG^* is the value for pure water. The free energy of activation for the solution becomes

$$\Delta G_o^* = \Delta G^* + \frac{18Cn(\nu_1 \delta_1 + \nu_2 \delta_2)}{1000d - CM + 18C(\nu_1 + \nu_2)} \quad (4.2-4)$$

Inserting this in equation (4.2-2) gives

$$\frac{D^{id}}{D^o} = \exp \left[- \frac{1}{RT} \left(\frac{18Cn(\nu_1 \delta_1 + \nu_2 \delta_2)}{1000d - CM + 18C(\nu_1 + \nu_2)} \right) \right] \quad (4.2-5)$$

In this equation the term $18C/[1000d-CM+18C(\nu_1+\nu_2)]$ is the species fraction of electrolyte. A plot of $\ln D^{id}/D_c$ against this factor should therefore give a straight line of slope $n(\nu_1\delta_1+\nu_2\delta_2)/RT$. The perturbation parameters δ_1 and δ_2 should be characteristic of the ions involved. By considering a number of electrolytes it should be possible to prepare a table of these parameters for various ions, from which diffusion coefficients for other electrolytes could be predicted.

4.3 Discussion

Figure 4.1 shows the concentration dependence of the mutual diffusion coefficient at the four temperatures studied. The concentration dependence is complex, showing a minimum at low concentrations (about 0.25 molar) and a shallow maximum at high concentrations (about 6 molar). A similar minimum at low concentrations is found for most electrolyte systems, but maxima such as that seen here for KOH are less common. The values of D shown for zero concentration are the theoretically calculated Nernst values. The experimental data are seen to extrapolate smoothly to this limit.

The empirical relationship $D = A\exp(\frac{C}{T})$, where A and C are constants, is frequently used to describe the temperature dependence of the diffusion coefficient. This relationship is tested for KOH solutions at constant composition in Figure 4.2, and is seen to be successful over the temperature range studied. The above equation may therefore be used for interpolating the data to other temperatures. It may also be used for extrapolation, to obtain D values for temperatures above 75°C , although with rather less confidence.

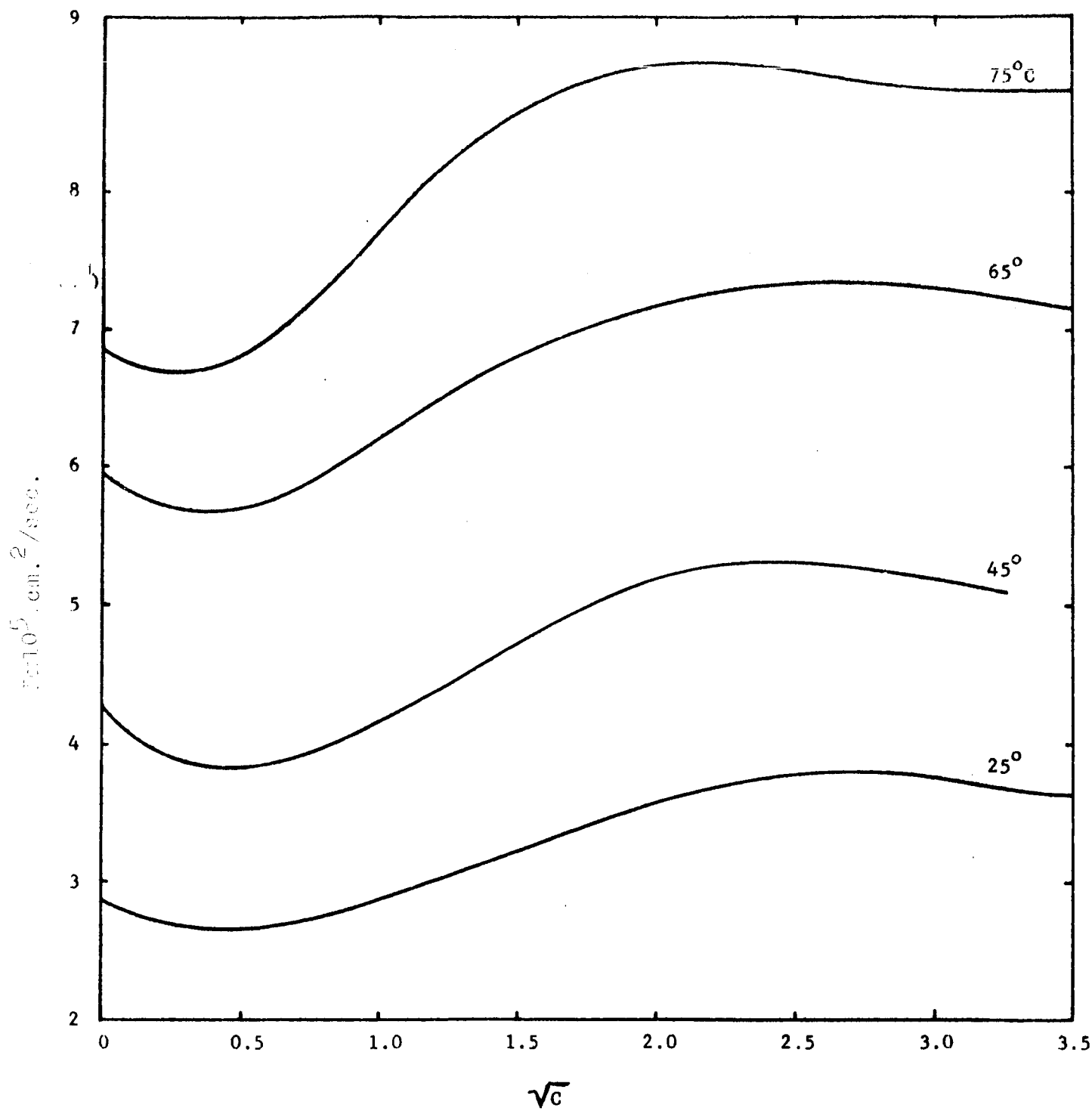


Figure 4.1 Diffusion coefficients of Aqueous KOH solutions

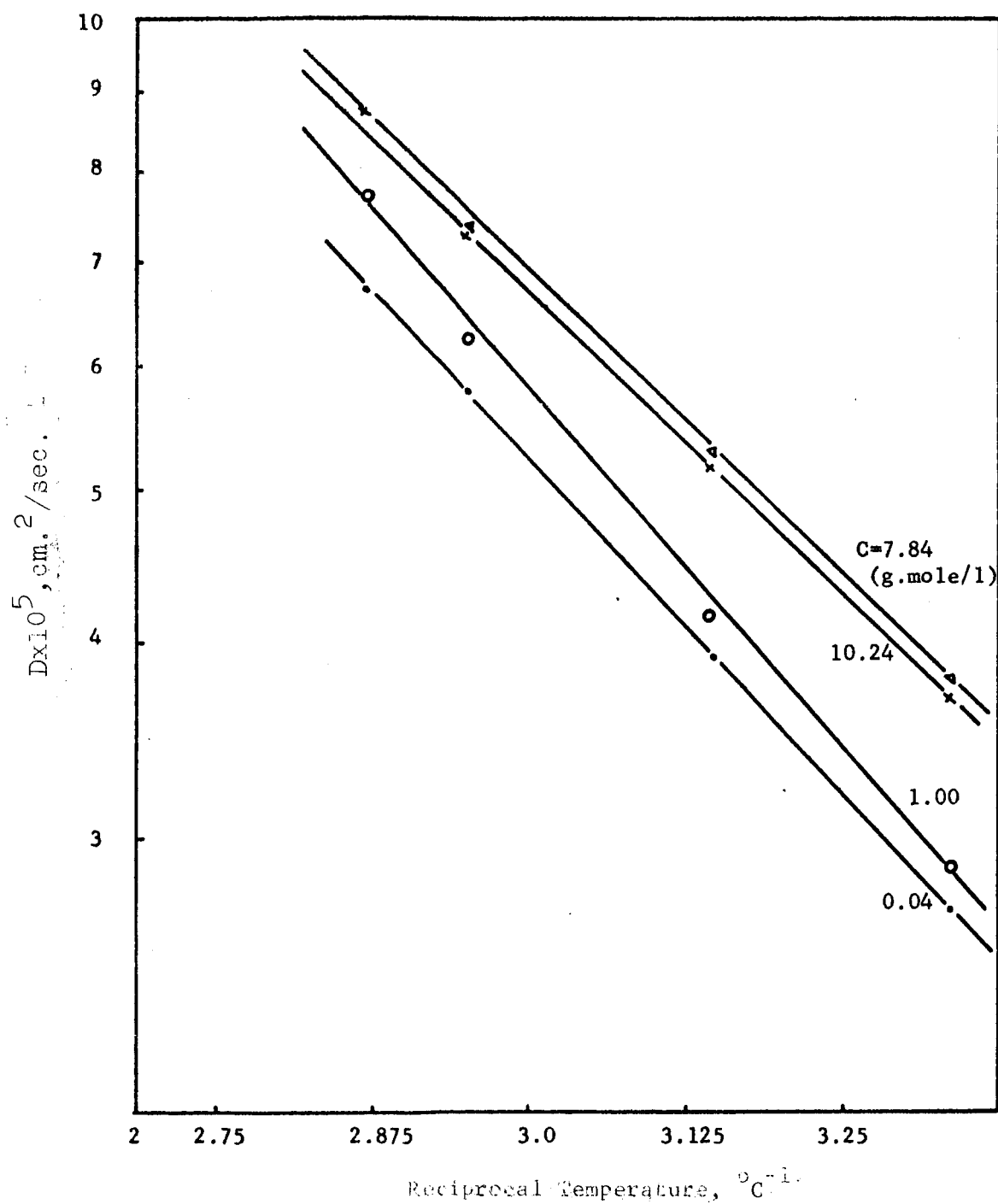


Figure 4.2 Log D versus T^{-1} for Aqueous KOH solutions

Figure 4.3 shows a semilog plot of D^{id}/D_w^0 vs species fraction of electrolyte. Values of the thermodynamic factor in Equation (4.2-1) were calculated using activity coefficients obtained from E.M.F. data (26). As suggested by the theory developed in the previous section, the plot is linear at electrolyte concentrations up to about 8N. From the slope of the line,

$$n(\delta_{K^+} + \delta_{OH^-}) = 2.325 \text{ cal. (g.mole}^{-1}\text{)}$$

Using this value for the perturbation parameter, theoretical values of the mutual diffusion coefficient may be calculated using Equation (4.2-4); these are compared with experimental data in Figure 4.4. The proposed model is seen to provide a much better fit than the Onsager-Fuoss theory at high concentrations. For the concentration range 0-10 g.mole/l., the average deviation between experiment and Equation (4.2-4) is 1.3%.

It is of interest to note that the simple theoretical model used above also applies well to other transport coefficients of potassium hydroxide solutions. Thus when the relative viscosity (η/η^0) and relative self-diffusion coefficient of water (D_w/D_w^0) are plotted vs. electrolyte species fraction on a semilog plot, straight lines are obtained (27). A similar concentration dependence is observed for the diffusion coefficient of oxygen in KOH solutions (see Figure 3.3).

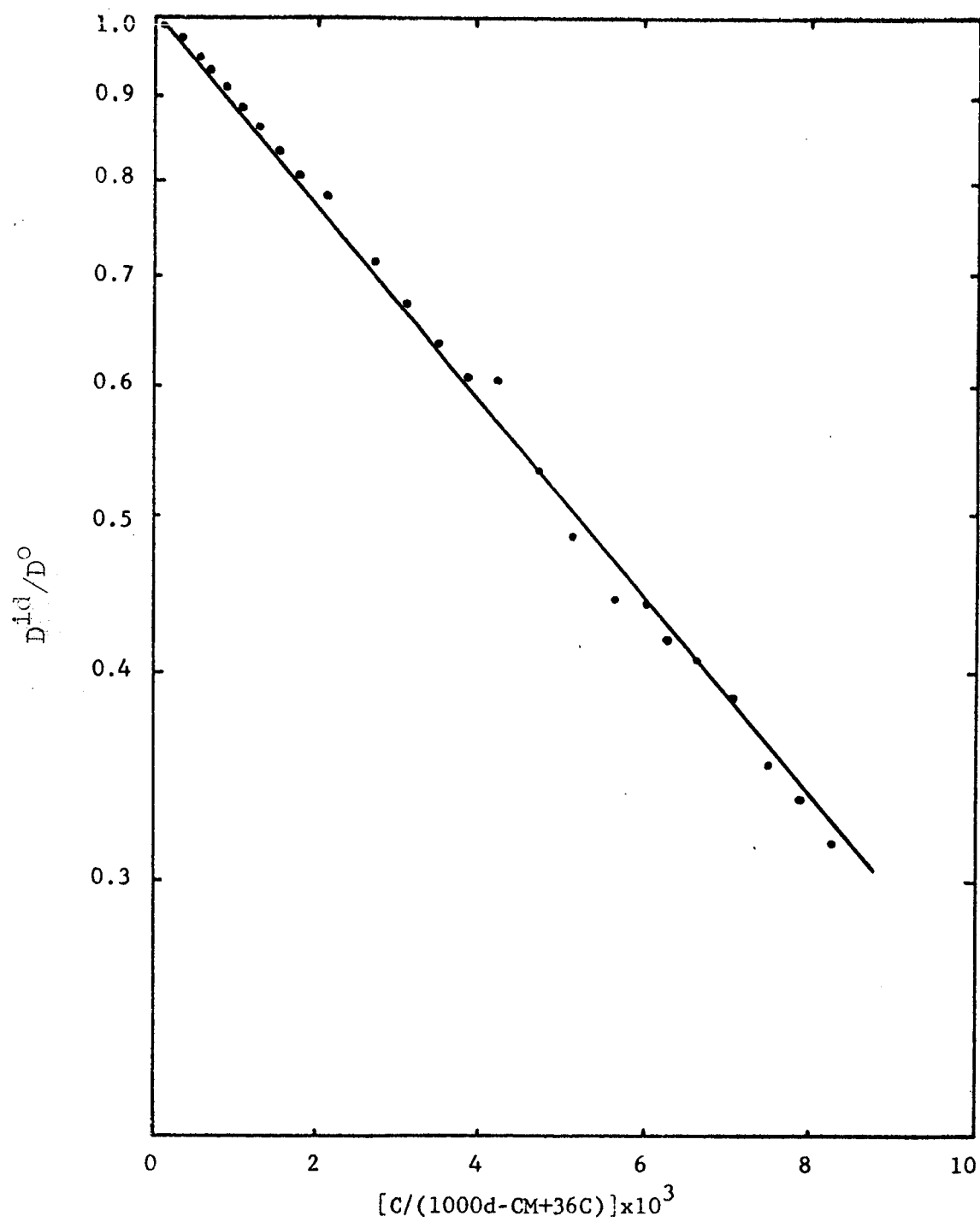


Figure 4.3 Relative diffusion coefficients D^{1d}/D^o for Aqueous KOH solutions at 25°C

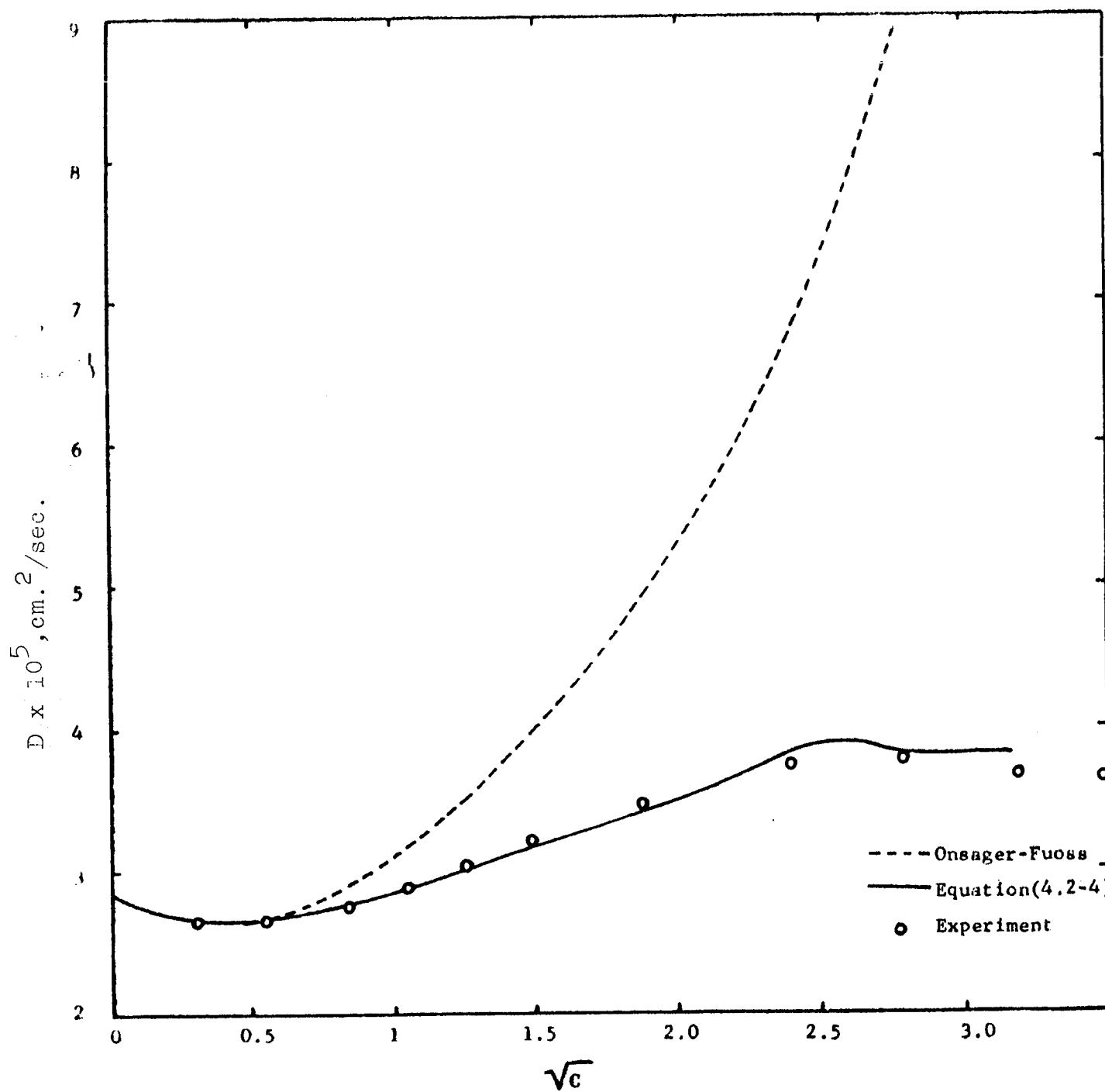


Figure 4.4 Diffusion Coefficients of Aqueous KOH Solutions at 25°C

5. LITERATURE SURVEY OF PROPERTIES OF LITHIUM HYDROXIDE SOLUTIONS J. Jolly

During this period a literature search has been made to determine what measurements of physical properties of lithium hydroxide solutions are available. The physical properties searched for have included density, solubility of lithium hydroxide, heat capacity, viscosity, electrical conductivity, and vapor pressure of the aqueous solutions; solubility and diffusivity of gases in aqueous solutions (no data were found); and properties of the solid. The literature searched has consisted of International Critical Tables, Landolt-Bornstein, Chemical Abstracts from 1927 to date, and miscellaneous handbooks.

The data found in these sources are summarized in Appendix 1.

6. Future Plans

For the next six months work will be concentrated on the following areas:

1. Completion of the solubility measurements at temperatures up to 100°C and saturated KOH.
2. Measurement of the diffusivity of hydrogen and oxygen in KOH solutions.
3. Measurement of both solubility and diffusivity of hydrogen and oxygen in LiOH solutions.
4. Further development of a theory of solubility for concentrated electrolytes.
5. Further development of a theoretical treatment of diffusion in concentrated electrolytes.
6. Place a more sensitive chromatograph into operation so as to permit more precise measurements of solubility and diffusivity at higher temperatures and alkali concentrations.

APPENDIX 1

Physical Property Values for LiOH Solutions from the Literature

A.1.1 Symbol and Units

Temperature will be expressed in $^{\circ}\text{C}$

LiOH concentration will be in weight %

Vapor pressure of LiOH solutions will be in mm. Hg.

Density will be in g/cc

Heat capacity, in Joules/g $^{\circ}\text{C}$

Viscosity in centipoises

Electrical conductivity in $\text{ohm}^{-1}\text{cm}^2$

A.1.2 Solubility of Lithium Hydroxide in Water (25,26)

<u>Temperature</u>	<u>Wt % LiOH</u>	<u>Temperature</u>	<u>Wt % LiOH</u>
-10.5 $^{\circ}\text{C}$	7.23	120 $^{\circ}\text{C}$	15.03
-18.0	11.20	140	14.38
0	10.64	150	14.23
10	10.80	160	13.79
20	10.99	180	13.19
25	11.14	190	12.81
30	11.27	205.5	12.43
40	11.68	265	11.89
50	12.12	295	12.35
60	12.76	321.6	13.04
80	14.21		
100	16.05		

Note: The solid phase in equilibrium with saturated solutions in the monohydrate $\text{LiOH}\cdot\text{H}_2\text{O}$

A.1.3 Vapor Pressure of LiOH Solutions (29,34,35)

<u>Temperature</u>	<u>Wt % LiOH</u>	<u>Vapor Pressure</u>	<u>Temperature</u>	<u>Wt % LiOH</u>	<u>Vapor Pressure</u>
20	2.338	17.002 mm.Hg	160	4.76	4403 mm.Hg
	4.569	16.469		8.59	4480
	6.701	15.932		13.04	4273
	8.739	15.368	200	4.76	11012
	10.69	14.794		8.59	10984
25	2.338	22.034		13.04	10728
	4.569	22.316	250	4.76	27981
	6.701	21.597		8.59	28058
	8.739	20.841		13.04	27231
	10.690	20.081	300	4.76	60656
100	0.0989	745.6		8.59	60605
	2.391	722.6		13.04	59777
	4.571	666.8	350	4.76	117795
	5.392	666.8		8.59	116760
	6.085	654.5		13.04	116916
120	4.76	1437			
	8.59	1437			
	13.04	1282			

A.1.4 Vapor Pressure of Solid LiOH.H₂O (37)

<u>Temperature</u>	<u>Vapor Pressure</u>
21.5 °C	3.1 mm.Hg
25.0	3.5
30.0	5.0
40.0	13.1
50.2	23.4
60.0	51.9
70.0	97.0
79.9	190.3
80.0	195.2
90.0	358.5

A.1.5 Heat Capacity of Aqueous LiOH Solutions at 20°C (31)

<u>Wt. %</u>	<u>Heat Capacity</u>
0.5	4.17 Joules/g.°C
1.0	4.12
2.5	4.06
5.0	3.99

A.1.6 Viscosity of LiOH Solutions (32)

<u>Temperature</u>	<u>Wt % LiOH</u>	<u>Viscosity</u>	<u>Temperature</u>	<u>Wt % LiOH</u>	<u>Viscosity</u>
20	1.18	1.139	50	1.18	0.61
	2.33	1.294		2.36	0.67
	4.55	1.686		4.61	0.86
	6.68	2.223		6.77	
	8.74	2.990		8.83	1.43
	10.81	4.084		10.92	
30	1.18	0.907	75	1.18	0.42
	2.34	1.028		2.37	0.46
	4.57	1.325		4.63	0.58
	6.72	1.720		6.80	
	8.77	2.255		8.86	0.88
	10.85	3.008			
40	1.18	0.743			
	2.35	0.841			
	4.59	1.069			
	6.75	1.368			
	8.80	1.758			
	10.89	2.305			

A.1.7 Density of LiOH Solutions (30)

Wt % LiOH	°C	0	10	20	25	30	40	50	60	80
1		1.0122	1.0115	1.0102	1.0090	1.0075	1.0041	1.0000	0.9958	0.9860
2		1.0240	1.0230	1.0217	1.0203	1.0188	1.0155	1.0114	1.0078	0.9973
4		1.0468	1.0456	1.0437	1.0422	1.0407	1.0371	1.0331	1.0286	1.0189
6		1.0690	1.0674	1.0650	1.0636	1.0621	1.0582	1.0541	1.0496	1.0397
8		1.0908	1.0888	1.0862	1.0867	1.0830	1.0790	1.0747	1.0701	1.0600
10		1.1125	1.1102	1.1074	1.1057	1.1038	1.0996	1.0952	1.0906	1.0803

A.1.8 Electrical Conductivity of LiOH Solutions (33)

<u>Wt % LiOH</u>	<u>Equivalent Conductance at 25°C</u>	<u>Specific Conductance at 25°C</u>
	cm. ² /ohm	$\frac{1}{\text{ohm cm}}$
10.83	79.7	0.3992
6.57	114.6	0.3352
5.00	129.0	0.2849
2.47	157.9	0.1640
1.16	178.3	0.0834
0.55	191.9	0.04432

at infinite dilution 237.2

0.008
(Extrapolated after plotting
the above values)

A.1.9 Properties of Solid Lithium Hydroxide (37)

<u>Properties</u>	<u>Monohydrate LiOH·H₂O</u>	<u>Anhydrous LiOH</u>
Molecular Weight	41.96	23-94
Crystal Structure	Monoclinic	Tetragonal
LiOH Content (theoretical)	57.07%	100%
Li ₂ O Equivalent	35.60%	62.41%
Density	1.51	1.46
Melting Point	Loses water @100-110°C VP at 25°C = 3.90 mm.	471.1°C
Heat Capacity(25°C)	19.00/cal/deg/mol	11.849/cal/deg/mol
Heat of Soln.(25°C)	-0.867 kcal/mol	-4.887 kcal/mol
Heat of formation (25°C)	-188.926 ± 0.12 kcal/mol	-116.589 ± 0.09 kcal/mol
Heat of fusion		5.01 kcal/mol
Free energy of formation (25°C)	-163.437 ± 0.16 kcal/mol	-105.676 ± 0.13 kcal/mol
Entropy	17.07 ± 0.05 cal/deg/mol	10.23 ± 0.5 kcal/deg/mol

List of References

1. Walker, R. D., Second Semi-Annual Report, October, 1966, NASA Research Grant NGR 10-005-022.
2. Gubbins, K. E., Carden, S. N., and Walker, R. D., J. of G. C., 3, 98 (1965).
3. Walker, R. D., First Semi-Annual Report, March 1966, NASA Research Grant NGR 10-005-022.
4. Geffcken, G., Zeit. Physik. Chemie, 49, 257(1904).
5. Tobias, C. W., Davis, R. E., and Horvath, G. L., Electrochimica Acta, 12, 287(1967).
6. Lange, A. L. (Ed.) Handbook of Chemistry, McGraw-Hill Book Co., New York (1961).
7. Knaster, M. B., and Apel'baum, L. A., Russian J. Phys. Chem., 38, 120(1964).
8. Walker, R. D., Third Semi-Annual Report, March, 1967, NASA Research Grant NGR 10-005-022.
9. Ruetschi, P., and Amile, R. F., J. Phys. Chem., 70, 718(1966).
10. Lannung, A., J. Am. Chem. Soc., 52, 68(1930).
11. Hildebrand, J. H., J. Chem. Phys., 20, 190(1952).
12. Morrison, T. J., and Johnstone, N. B., J. Chem. Soc., 3441(1954).
13. Pierotti, R. A., J. Phys. Chem., 67, 1840(1963).
14. Elley, D. D., Trans. Faraday Soc., 40, 184(1944).
15. Koithoff, I. M., and Lingane, J. J., Polarography, Vol. 1, p. 25, Interscience (1952).
16. von Stackelberg, H., Pilgrim, M., and Toome, V., Z. Electrochem., 57, 342(1953).
17. Gubbins, K. E., and Walker, R. D., J. Electrochem. Soc., 112, 469 (1965).
18. Meites, L., and Meites, T., J. Am. Chem. Soc., 73, 395(1951).
19. Lingane, J. J., and Loveridge, J., ibid., 72, 438(1950).

20. Walker, R. D., Third Semi-Annual Report, March, 1967, NASA Research Grant NGR 10-005-022.
21. Chang, P. and Wilke, C. R., J. Phys. Chem., 59, 592(1955).
22. Onsager, L. and Fuoss, R. M., J. Phys. Chem., 36, 2689(1932).
23. Glasstone, S., Laidler, K. J. and Eyring H., "The Theory of Rate Processes", McGraw-Hill, New York (1941).
24. Podolsky, R. J., J. Am. Chem. Soc., 80, 4442(1958).
25. Hildebrand, J. H. and Scott, R. L., "Regular Solutions", Prentice-Hall, Engelwood Cliffs, N. J. (1962).
26. Harned, H. S. and Cook, N. A., J. Phys. Chem., 59, 496(1937).
27. McCall, D. W. and Douglass, D. C., J. Phys. Chem., 69, 2001(1965).
28. Seidell, Solubilities of Inorganic and Metal Organic Compounds, Van Nostrand Co., New York (1940).
29. Stephen, Miller, J. Chemical Eng. Data I, 501(1962).
30. International Critical Tables 3, 76(1929).
31. International Critical Tables 5, 123(1929).
32. International Critical Tables 5, 15(1929).
Hitchcock, I., Ing. Eng. Chem., 29, 302(1937).
33. Darken, M., J. Am. Chem. Soc., 64, 621(1942).
34. Walther, Groeneveld, Z. fur Physik, Chem., 32, 110(1962).
35. Foote Mineral Co., Technical Bulletin.
36. Back, R. O., and Beardman, W. W., Jr., Chimia, 18, 110(1964).
37. Lithium Corporation of America, Inc.
Technical Bulletin 101-162.